2014

The Electrochemical Detection Of Explosive Compounds Using Polymer And Chemically Modified Electrodes

Hollis Rachial D
North Carolina Agricultural and Technical State University

The Electrochemical Detection of Explosive Compounds Using Polymer and Chemically Modified Electrodes

Rachial D Hollis

North Carolina A&T State University

A thesis submitted to the graduate faculty

in partial fulfillment of the requirements for the degree of

MASTER OF SCIENCE

Department: Chemistry

Major: Chemistry

Major Professor: Dr. William Adeniyi

Greensboro, North Carolina

2014

The Graduate School
North Carolina Agricultural and Technical State University
This is to certify that the Master's Thesis of

Rachial D Hollis

has met the thesis requirements of
North Carolina Agricultural and Technical State University

Greensboro, North Carolina
2014

Approved by:

Dr. William Adeniyi
Major Professor

Dr. Alex Williamson
Committee Member

Dr. Zerihun Assefa
Committee Member

Dr. Margaret Kanipes-Spinks
Department Chair

Dr. Sanjiv Sarin
Dean, The Graduate School

Biographical Sketch

God gifted Rachial D Hollis to the world on August 12, 1990 in Columbia, South Carolina. She is more recently from Orange, Virginia. She has a dog, Hemingway.

Rachial graduated from Gardner-Webb University in May 2012 with a Bachelor of Science, Chemistry. She is a candidate for the Master of Science degree at North Carolina A&T State University.

Dedication

I dedicate this work to the most supportive parents in the world, Trish and Andrew Dahl. I also extend that dedication to Grams and John Freeman, and the rest of my family. Thank you all for your support, encouragement, and love.

Acknowledgements

I acknowledge the grace of God and the power of prayer, without these things I would not have made it this far. Thanks to Rhecia Goodley and all of the graduate students in the Chemistry department for making these two years far more enjoyable than they ever had to be. Thanks to my committee members, Dr. Williamson and Dr. Assefa, for the encouragement and direction. Finally, paltry words would never do to express the gratitude I have for my advisor Dr. Adeniyi. He taught me how to be a chemist and I will owe him my career.

Table of Contents

List of Figures

List of Tables

Abstract

The detection and quantification of explosive compounds is extremely important in global security, antiterrorist, and forensic activity. While there are sensitive and reliable methods for detection, the development of electrochemical techniques is used here because they are simple, affordable, and can be made for field use. In this investigation, chlorogenic acid (CGA) modified glassy carbon electrode (GCE) was used to detect hydrazine in concentrations as low as 0.05mM; aspartic acid modified GCE was used to detect both nitrobenzene and 4-nitrotoluene in concentrations as low as 3.3μM and 1.3μM, respectively; and finally phenol red coated GCE was used to detect nitrobenzene in concentrations as low as 3.3μM. The CGA modified GCE showed high redox activity at a pH of 7.5 and could detect hydrazine at scan rates as high as 100mV/s. The aspartic acid coated electrode showed high redox activity between a pH of 5.01 and 6.84 and could detect the nitrobenzene and 4-nitrotoluene at scan rates as high as 100mV/s. The phenol red coated electrode was effective between pH of 5-6 and could detect the nitrobenzene at scan rates as high as 130mV/s. Effects of surfactants such as SDS, DTAB, and DTAC were studied on analytes and their electrochemical activities observed. Overall, the surfactants showed a decrease effect in the current density. The durability of these films on electrodes was also studied. Both the CGA and aspartic acid films showed an immediate and steady decrease in function as successive scans were carried out. This decrease in function could be attributed to degeneration of thin coatings of the film with time. Phenol red coated GCE showed good stability for 15 scans.

CHAPTER 1

Introduction

Nitro-aromatic and other nitrogen containing compounds have many applications including dyes, polymers, pesticides, and explosives. Due to the properties specific to these nitrogen compounds, decomposition in the environment can be difficult and therefore cause accumulation. Since nitrogen compounds are mostly man-made and not naturally occurring, the fate of these compounds is of great interest.[1]

There are serious implications associated with the presence of nitrogen compounds in the environment: they can either be reactive as explosives, or their accumulation as a result of runoff from industrial sources could pose a potential threat to human health.

The explosive nature of nitro compounds is enhanced by their capability to undergo rapid nuclear or chemical composition. The widespread terrorist activities in the form of bombings to buildings, buses, trains and military establishments made nitro and other explosive compounds curious and aggressive targets of scientific investigations.

A wide variety of explosives have been characterized by Singh[2] in accordance to their structures and performance as shown in Figure 1 below.

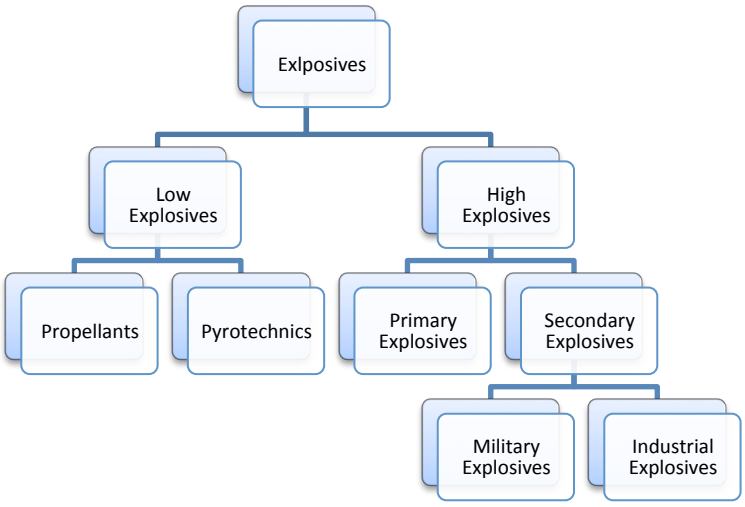

Figure 1. Characterization of Explosive Compounds.

Nitrogen-containing compounds, which are the target of this investigation, include nitro-aromatics and nitro-amines. They feature prominently at military sites, which are more exposed to secondary than primary explosives. The abundance of nitrogen-containing compounds makes this class of compounds readily available for terrorist activities. This investigation, therefore, will target the detection of explosives categorized as secondary explosives.

The development of techniques for the detection and quantification of explosives has become extremely important in global security, antiterrorist, and forensic activities. The increasing escalation of terrorism has led to increasing efforts in the development of innovative and effective sensors to monitor explosives.[3]

Some methods that have been developed to monitor these potentially dangerous compounds include gas and liquid chromatography[4], spectrophotometry[5], fluorometry[6], laser-induced breakdown spectroscopy (LIBS)[7], electrochemical[8] and others.[9]

Whereas many methods have been developed for the detection of explosives, electrochemical sensors are advantageous over other available techniques. Detection by canine suffers from the high cost of maintenance and periodic exhaustion of the domestic animal. Some

studies[9] show that sniffing dogs are not sensitive to certain chemical smells. Most of the other methods available for detection of explosives are getting increasingly ineffective because of the amount of materials used in making bombs. In addition, most instrumentation used in methods other than electrochemistry is bulky, expensive, and rather sophisticated to handle. The need for a sensitive, economical and portable instrument gives electrochemical methods some advantages:

i) Electrochemical instruments are generally inexpensive, simple, and can be miniaturized to detect homemade bombs.[10]

ii) A careful choice of electrode materials makes it possible to design the method so that specific explosive molecules could be targeted.

iii) By carefully selecting potentials and currents, sensitivity of the method could be enhanced in order to attain low detection limits.

iv) Results are obtained much faster than most other instrumental techniques

v) Electrochemical methods of detection promises some specificity

vi) Generally, the inherent redox properties of nitroaromatic explosives make them ideal candidate for electrochemical detection.

As a result of the chemical moiety of these nitrogen-containing molecules, this investigation has focused on specific examples identified below.

1.1 Hydrazine.

1.1.1 Characterization and Applications. Hydrazine seen below in Figure 2 is an alkali compound with two nitrogen atoms bonded together with a lone pair and two hydrogen atoms on each nitrogen.

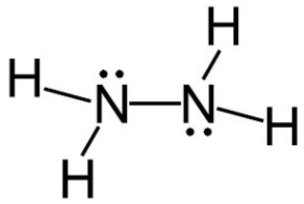

Figure 2. Hydrazine Structure.

Hydrazine is a colorless liquid at room temperature. The compound is both combustible and explosive in particular when catalyzed by metals and their oxides.[11] The decomposition of hydrazine is rapid with a high-energy yield. The compound has a low molecular weight of 32.05 g/mol and yields gaseous products such as ammonia, nitrogen, and hydrogen at high temperatures. This makes hydrazine products ideal for use as rocket fuel by organizations such as the National Aeronautics and Space Administration (NASA) and the United States Air Force.[12]

1.1.2 Exposure and Toxicity. The only reported natural source of hydrazine is the tobacco plant.[11] Hydrazine can be released into the air, soil, and water by discharge during improper storage, handling, transport, and waste disposal. A common method that has been used to dispose hydrazine is dilution with water and addition of sulfuric acid or hydrogen peroxide.

When exposed to aquatic life, hydrazine can be toxic. The dose required to kill half the test population (LD50) levels for certain fish species have been reported as low as 0.54mg/L and as low as 0.00008mg/L for aquatic microorganisms. Hydrazine is toxic to plants in both air and water and can inhibit plant germination.[11]

Humans can encounter hydrazine occupationally and accidentally. Effects of acute poisoning include nausea, vomiting, respiratory tract irritation, temporary blindness, pulmonary edema, seizures, and coma. Damage can occur to the liver, kidneys, and central nervous system.[13] Exposure to hydrazine can result in tumors incidences in the nose, lung, and liver. In a study of multiple in vitro systems including plants, phages, bacteria, fungi, and mammalian, hydrazine induced gene mutations and chromosome aberrations.[11]

1.2 4-Nitrotoluene.

1.2.1 Characterization and Applications. 4-Nitrotoluene as seen below in Figure 3 is a benzene ring with a nitro (NO_2) group at the 1 position and a methyl (CH_3) group at the 4 position on the ring.

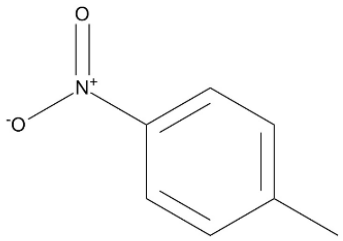

Figure 3. 4-Nitrotoluene Structure.

4-Nitrotoluene is used in the dye industry as azo and sulfur dye intermediates, and the explosives industry as dinitrotoluene and trinitrotoluene intermediates.[14]

4-Nitrotoluene exists as a vapor in ambient air and can also be found in soil and water sources that have been exposed. The degradation reaction of 4-Nitrotoluene with photochemically produced hydroxyl radicals in air has a half-life of 21 days. Volitilization is an important fate of 4-Nitrotoluene found in soil and water. Degradation can also occur during the treatment of wastewater.[14]

1.2.2 Exposure and Toxicitiy. The most likely route of exposure to 4-Nitrotoluene is dermal exposure by workers where it is produced or used. General populations surrounding sites of production and use may also be exposed by inhalation of ambient air or consumption of drinking water.[14]

4-Nitrotoluene causes irritation to the eyes, skin, and respiratory tract. There has not been extensive research in the evaluation of its carcinogenic properties in humans or animals. Exposure to 4-Nitrotoluene causes methemoglobinemia which results in decreased blood oxygen content and can cause complications ranging from headaches and dizziness to seizures and coma.[14]

1.3 Nitrobenzene.

1.3.1 Characterization and Application. Nitrobenzene, as seen below in Figure 4, is a benzene ring with a nitro (NO_2) group, produced by nitration of benzene with fuming nitric acid.

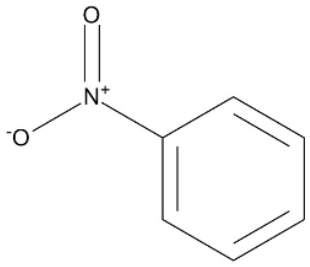

Figure 4. Nitrobenzene Structure.

It is a colorless liquid at room temperature. It is a fire hazard with an explosive limit of 1.8% volume in air.[15] There is no reported natural occurrence of nitrobenzene. However, it has been shown that benzene can react with nitrogen oxides to produce nitrobenzene as seen below in Figure 5.

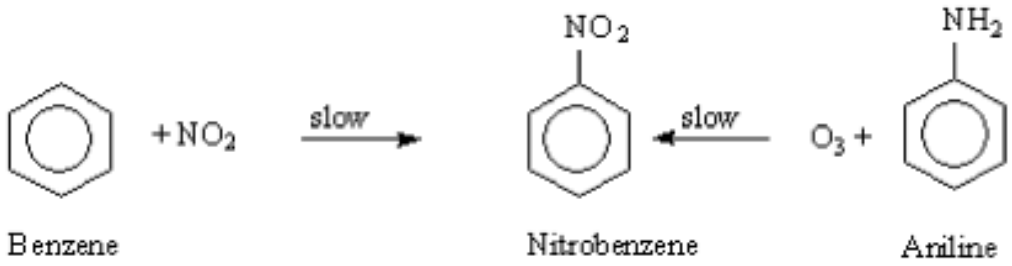

Figure 5. Production of nitrobenzene in the atmosphere.

Also under the same atmospheric conditions, aniline can be oxidized by ozone to form nitrobenzene.[15] Up to 98% of the nitrobenzene produced in the United States is used for the synthesis of aniline which is principally used to make polyurethanes.[15]

1.3.2 Exposure and Toxicity. Concentrations of nitrobenzene in the environment are generally low, as most of it is used in a closed system to produce aniline and significant loss in the process is unlikely. Therefore, populations living near petroleum refinery plants, hazardous waste sites, and manufacturing sites are at risk for significant exposure to nitrobenzene through air, soil, and groundwater contamination.[15]

Nitrobenzene is toxic to humans by exposure to the skin, inhalation, and ingestion. Exposure to nitrobenzene can cause neurotoxic symptoms such as headache, nausea, apnea, and coma, as well as damage to the liver and spleen. However, the main systemic effect to nitrobenzene exposure is methemoglobinaemia.[15]

CHAPTER 2

Literature Review

Polymers are used to coat the surface of the solid state electrodes because the electron donating nature of most polymers is advantageous in detecting electron accepting nitroaromatic compounds. There has been much research[16] on different types of modified electrodes and their functions. However the modifiers in this investigation have not been widely used for these purposes so there is little information about their behavior.

Previous studies have been conducted using chlorogenic acid to modify an electrode in the detection of hydrazine. Golabi and Zare[16a] used a method of electrode preparation similar to the one used in this study. Their coated electrode performed optimally at pH 6-9 buffers, with any pH lower than 6 showing a decrease in sensitivity. The lowest detected hydrazine concentration was 0.05mM.

Salimi and Hallaj reported a electroless deposition of chlorogenic acid on a carbon ceramic composite electrode using a sol-gel procedure. According to their reports on pH dependence, a pH of 5 was found to be unstable. The lowest concentration tested in their study was 0.1mM. Their results indicated that their process of coating the electrode was fast and stable.[17]

Aspartic acid has also been used to modify electrodes for detection of explosive compounds. Wang et al reported using an aspartic acid coated electrode to detect 2,4-dinitrophenol and 2,5-dinitrophenol. They were able to detect concentrations as low as 1.1μM and 0.7μM, respectively. Also, they found that there was a decrease in electrode function at pH values above 6 due to a deficiency of protons in the reduction reaction. Furthermore, there was a

linear correlation between scan rate and peak current, indicating that the detection of these compounds was an adsorption-controlling process.[18]

Aspartic acid coated electrode has also been used for the detection of biologically important entities. One report cites the use of an aspartic acid coated electrode for the detection of dopamine concentrations as low as 1.2μM in the presence of ascorbic acid. The differentiation between dopamine and ascorbic acid interaction on the electrode was attributed to charge discrimination that favored the interactions of the negatively charged groups on the electrode and dopamine.[16c]

Phenol red has no known applications for detection of explosive compounds. It has been reportedly used as a biosensor to detect NAD+/NADH redox activity as it relates to the study of enzymes.[16b]

Yang, et al. reported using a phenol red modified glassy carbon electrode to detect trace lead (II).[19] Using differential pulse anodic stripping voltammetry, lead (II) was detected in concentrations as low as 2.0×10^{-9} M. Their method of detection was applied successfully to the analysis of wastewater.

CHAPTER 3

Methodology

3.1 Instrumentation.

The BAS 100B electrochemical workstation was the primary instrument used in this investigation. Cyclic voltammetry (CV) was the primary electrochemical study used. Glassy carbon and gold electrodes were used in this investigation. A TR-403 Denver Instrument Company electronic balance was used for all measurements of mass. A Fisher Scientific AB15 pH meter was used for all measurements of pH.

3.2 Reagent Preparation.

The following solutions were prepared for use in this investigation. All chemicals were of analytical grades: sodium bicarbonate ($NaHCO_3$), sulfuric acid (H_2SO_4), aspartic acid, phenol red, nitrobenzene, 4-nitrotoluene, hydrazine, dodecyltrimethylammonium chloride (DTAC), dodecyltrimethylammonium bromide (DTAB), dodecyl sulfate sodium (SDS), monosodium phosphate, sodium hydroxide (NaOH), and sodium acetate.

1) 0.1 M $NaHCO_3$: An accurately weighed amount of 0.84g of $NaHCO_3$ was dissolved in a minimum amount of deionized water and diluted to 100mL in a volumetric flask.
2) 0.5 M H_2SO_4: 2.7mL of concentrated H_2SO_4 (18M) was measured with a pipet. It was transferred to a 100mL volumetric flask and diluted to the mark with deionized water.
3) 1.0×10^{-3} M Aspartic Acid: An accurately weighed amount of 0.013g of D-aspartic acid was dissolved in a minimum amount of deionized water and diluted to 100mL in a volumetric flask.

4) 0.1 Phenol Red: An accurately weighed amount of 3.764g of phenol red was dissolved in a minimum amount of deionized water and diluted to 100mL in a volumetric flask.
5) 0.5 M Nitrobenzene: 5mL of 99% reagent grade nitrobenzene (d= 1.204) was measured with a pipet. It was transferred to a 100mL volumetric flask and diluted with absolute ethanol to the mark. The solution was thoroughly mixed and stored in a plastic bottle.
6) 0.2M 4-Nitrotoluene: An accurately weighed amount of 2.74g of 4-nitrotoluene were dissolved in a minimum amount of ethanol and diluted to 100mL in a volumetric flask.
7) 0.5M Hydrazine: 2.8mL of a 55% reagent grade hydrazine solution was measured with 2500µL and 100µL pipets and transferred to a 100mL volumetric flask. It was diluted to the mark with deionized water. The solution was thoroughly mixed and stored in a plastic bottle.
8) 0.1M Dodecyltrimethylammonium chloride (DTAC): 2.63g of DTAC were accurately weighed and dissolved in a minimum amount of deionized water and diluted to 100mL in a volumetric flask.
9) 0.1M Dodecyltrimethylammonium bromide (DTAB): An accurately weighed amount of 2.09g of DTAB were dissolved in a minimum amount of deionized water and diluted to 100mL in a volumetric flask.
10) 0.1 M Dodecyl sulfate sodium (SDS): 2.88g of SDS were accurately weighed and dissolved in a minimum amount of deionized water and diluted to 100mL in a volumetric flask.

11) 0.15M Phosphate Saline Buffer Solution (PBS) pH 7.4: 24g of monosodium phosphate were dissolved in about 200 mL of deionized water. The pH was adjusted to 7.4 using sodium hydroxide and the total volume was brought to 1L with deionized water.
12) 0.15M PBS pH 6.8: 24g of monosodium phosphate were dissolved in about 200 mL of deionized water. The pH was adjusted to 6.8 using sodium hydroxide and the total volume was brought to 1L with deionized water.
13) 0.1 M HAc-NaAc Buffer pH 10: 4.2g of anhydrous sodium acetate were dissolved in about 200mL of deionized water. The pH was adjusted to 10 using sodium hydroxide and the total volume was brought to 500mL with deionized water.

3.3 Electrochemical Cell.

All electrochemical measurements were carried out in a glass cell in which a three-electrode system was inserted, including a working electrode, a counter electrode, and a silver-silver chloride (Ag/AgCl) reference electrode. The working electrode is the electrode at which the electrochemical reaction takes place. The counter electrode acts to complete the circuit of the potential applied to the working electrode. The Ag/AgCl reference electrode provides a known standard potential against which to measure changes at the working electrode. The electrodes were connected to the BAS 100 analyzer through a system of wires.

3.4 Electrode Cleaning.

All working electrodes were cleaned to enhance their sensitivity. Working electrodes were polished with a 0.05 micron alumina slurry and sonicated in concentrated nitric acid for at least 3 minutes. It was then rinsed with deionized water before use. Reference electrodes were stored in a reference electrode storage solution and rinsed with deionized water before use.

Counter platinum electrodes were frequently cleaned by rinsing with concentrated nitric acid or burning in a flame, then rinsed with deionized water before use.

3.5 Electrode Coating and Electrochemical Tests.

3.5.1 Chlorogenic Acid Coated Electrode.

3.5.1.1 Preparation. The cleaned and polished working electrode was activated in a 0.1 M $NaHCO_3$ solution. Cyclic voltammetry (CV) was performed from -1.10V to 1.60V for 40 cycles at a scan rate of 50 mV/s. The electrode was rinsed with deionized water and placed in a 1mM solution of Chlorogenic Acid (CGA) and 1.8mM acetic acid in 0.15M phosphate buffered saline (PBS) pH 7.5. The electrode was coated by performing CV from 0 to 0.9V for 32 cycles at a scan rate of 20 mV/s.

3.5.1.2 Voltammetric measurements of hydrazine, 4-nitrotoluene, and nitrobenzene. Samples of hydrazine, 4-nitrotoluene, and nitrobenzene were tested by placing the coated gold or glassy carbon electrode in a 0.15M PBS solution with the sample and performing CV from -0.2V to 0.85V for 3 cycles at a scan rate of 25 mv/s.

3.5.2 Aspartic Acid Coated Electrode.

3.5.2.1 Preparation. The cleaned and polished electrode was rinsed with deionized water and sonicated for three minutes in absolute ethanol. The electrode was rinsed with deionized water and placed in a 1x10-3 M aspartic acid solution. Cyclic voltammetry was performed from -1.2V to 1.9V for 25 cycles at a scan rate of 20mV/s. The coated electrode was rinsed with an ethanol/deionized water mixture and sonicated for three minutes in PBS pH 6.8.

3.5.2.2 Voltammetric measurements of hydrazine, 4-nitrotoluene, and nitrobenzene. Samples of hydrazine, 4-nitrotoluene and nitrobenzene were tested by placing the coated gold or

glassy carbon electrode in a 0.1M sodium acetate-acetic acid buffer with the sample and performing CV from -0.8V to 0.3V for 3 cycles at a scan rate of 25 mV/s.

3.5.3 Phenol Red Coated Electrode.

3.5.3.1 Preparation. The cleaned and polished electrode was rinsed with deionized water and activated in a 0.5M sulfuric acid solution. Cyclic voltammetry was performed from -0.5V to 1.4V for 20 cycles at a scan rate of 100 mV/s. The electrode was rinsed with deionized water and placed in a 0.05M PBS pH 7.5 solution with 5mM phenol red. Cyclic voltammetry was performed from 0V to 2V for 60 cycles at a scan rate of 100 mV/s.

3.5.3.2 Voltammetric measurements of nitrobenzene. Samples of nitrobenzene were tested by placing the coated gold or glassy carbon electrode in a 0.15M PBS solution with the sample and performing CV from -0.65V to 0.5V for 3 cycles at a scan rate of 100 mV/s.

3.6 Parameters Studied.

The following parameters were studied to find the optimal conditions at which detection occurred and determine which coating gave low detection limits.

1) Effect of concentration on electrode performance: different concentrations were introduced to the cell and the currents produced were recorded to create a calibration curve.
2) Effect of pH on electrode performance: tests were preformed at different pH values that were held constant by buffer solutions to determine which pH yielded the best results for each coated electrode.
3) Effect of scan rate on electrode performance: the scan rate at which the test was performed was varied to determine which scan rate yielded the best results for each coated electrode.

4) Effect of surfactant on electrode performance: three different surfactants were added to the test solution at increasing concentrations to measure the interference of the electrode performance.
5) Electrode durability: the sustainability of the electrodes coating was tested by running repetitive tests on the same electrode.

CHAPTER 4

Results

4.1. Glassy Carbon Electrode.

Hydrazine, nitrobenzene, and 4-nitrotoluene were all successfully detected by coated glassy carbon electrode. The results of these studies are detailed below.

4.1.1 Hydrazine on Modified GCE. Glassy carbon electrode was coated with CGA as described in Chapter 3. Cyclic voltammograms run before and after the addition of hydrazine are shown in Figure 6.

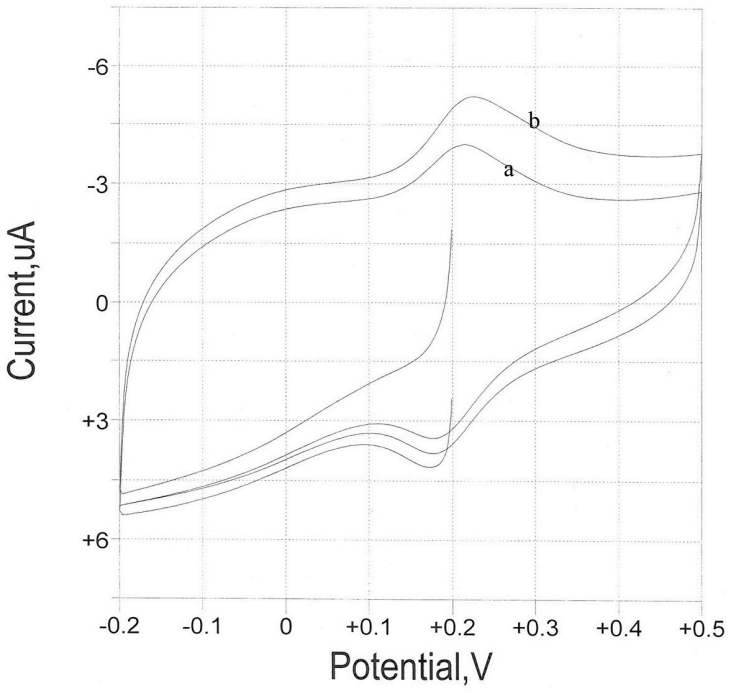

Figure 6. Cyclic voltammograms of a CGA modified GCE at 25mV/s in 0.15M PBS at pH 7.5. (a) without hydrazine (b) in the presence of 0.05mM hydrazine.

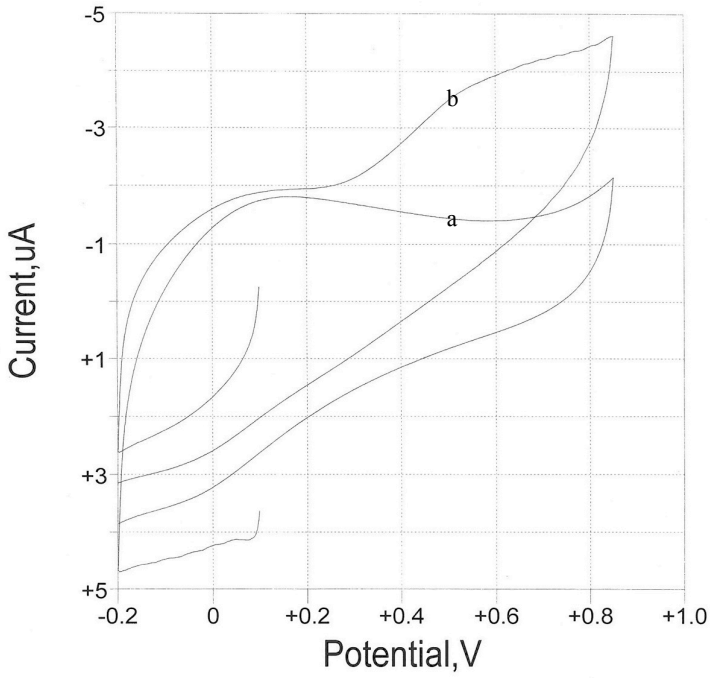

Figure 7. Cyclic voltammograms of (a) bare GCE in 0.15M PBS of pH 7.5 at 25mV/s (b) bare GCE in 0.15M PBS of pH 7.5 with 0.05mM hydrazine at 25mV/s.

As shown in Figure 6, the two peaks showing catalytic oxidation (223mV) and reduction (187mV) are separated by 36mV. However, the separation of the two peaks without hydrazine is 28mV. Figure 7 shows there are no oxidation or reduction peaks in the voltammograms of the uncoated GCE with and without hydrazine. This suggests that at GCA modified GCE, the oxidation of hydrazine to nitrogen occurs at a potential where oxidation is not observed at the bare GCE.

4.1.1.1 Effect of Hydrazine Concentration. Figure 8 shows the cyclic voltammograms obtained for different concentrations of hydrazine. Hydrazine concentrations are tabulated in Table 1. The calibration curve constructed from the voltammograms is shown in Figure 9.

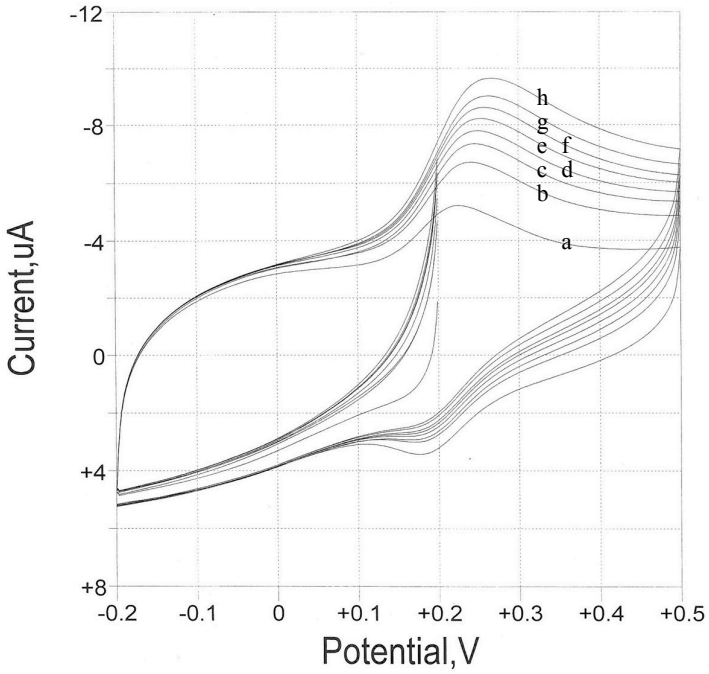

Figure 8. Cyclic voltammogram response of a CGA modified electrode at 25mV/s in 0.15M PBS pH 7.5 in the presence of (a) 0.05mM, (b) 0.125mM, (c) 0.15mM, (d) 0.175mM, (e) 0.2mM, (f) 0.225mM, (g) 0.25mM, (h) 0.275mM hydrazine.

Table 1

Concentration of hydrazine on CGA Coated GCE as seen in Figure 8, with data points for 0.075mM, 0.1mM, and 0.3mM.

Hydrazine Concentration (mM)	Ip_a ($x10^{-6}$ A)
(a) 0.05	1.77
0.075	2.11
0.1	2.37
(b) 0.125	2.54
(c) 0.15	3.09
(d) 0.175	3.26
(e) 0.2	3.52
(f) 0.225	3.79
(g) 0.25	4.10
(h) 0.275	4.53
0.3	4.82

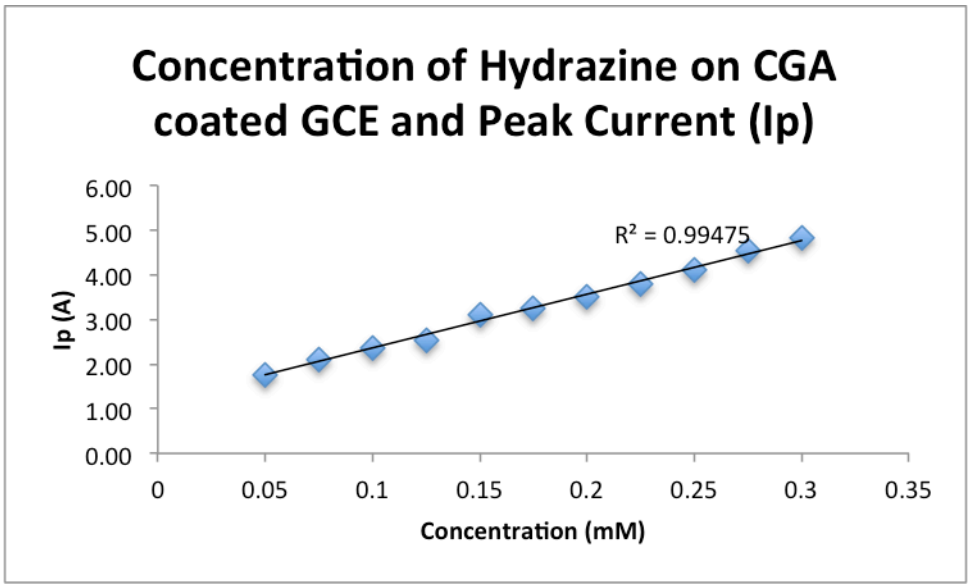

Figure 9. Concentration of hydrazine on CGA coated GCE in 0.15M PBS pH 7.5 at 25mV/s.

The calibration curve in Figure 9 shows a linear relationship between the current density and hydrazine concentration with a good linear regression of 0.99475. The regression analysis with a low sensitivity of 0.05mM of hydrazine offers good precision and a low detection limit with this method. Electrocatalytic oxidation of hydrazine on CGA modified electrode by cyclic voltammetry had been investigated by S.M. Golabi and H.R. Zareb[16a] and a similar detection limit is achieved in this work. This work shows that the method could be used for both qualitative and quantitative detection of hydrazine.

4.1.1.2 Effect of Scan Rate. In Figure 10, the cyclic voltammograms of a CGA modified glassy carbon electrode shows the effect of current density at different scan rates. The peak current for the oxidation of hydrazine is plotted against the square root of the scan rate and shown in Figure 12.

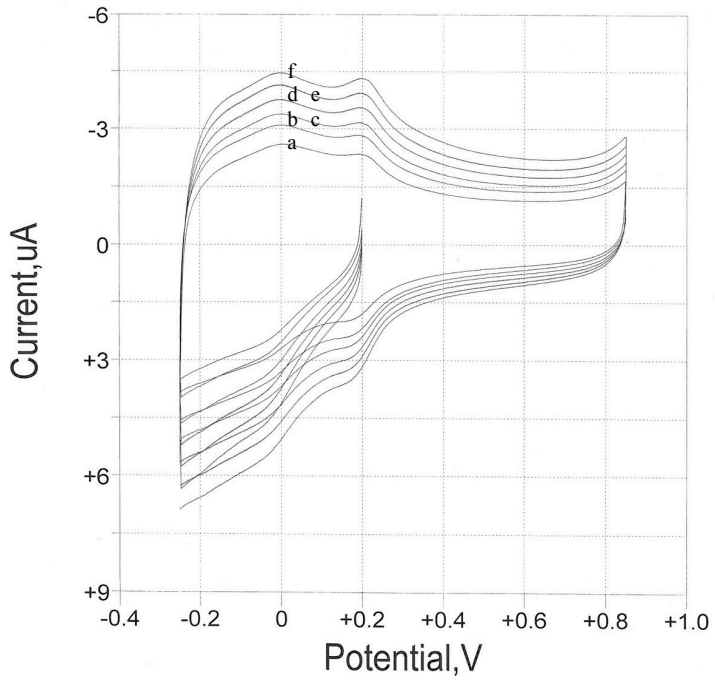

Figure 10. Cyclic voltammograms of CGA modified glassy carbon electrode at various scan rates in 0.15M PBS pH 7.5. Scan rates shown here are a) 50, b) 60, c) 70, d) 80, e) 90, and f) 100mV/s.

Table 2.

The effect of scan rate on the CGA modified GCE

Scan Rate (mV/s)	Scan Rate$^{1/2}$	Ip_a (x10^{-7} A)
(a) 50	7.1	0.21
(b) 60	7.7	0.553
(c) 70	8.4	0.999
(d) 80	8.9	1.37
(e) 90	9.5	1.83
(f) 100	10	2.4

Table 2 and Figure 10 show that both anodic and cathodic currents increase directly to the scan rate for scan rates between 50 and 100 mV/s. This behavior suggests possible facile charge transfer. Upon addition of hydrazine to the solution, there is an enhancement of the

anodic current. Figure 10 also shows that the catalytic oxidation peak slightly changes to a more positive potential. Figure 10 gives a linear graph in the plot of scan rate against the peak current, seen in Figure 11, and a standard deviation of 8.1321×10^{-8} A.

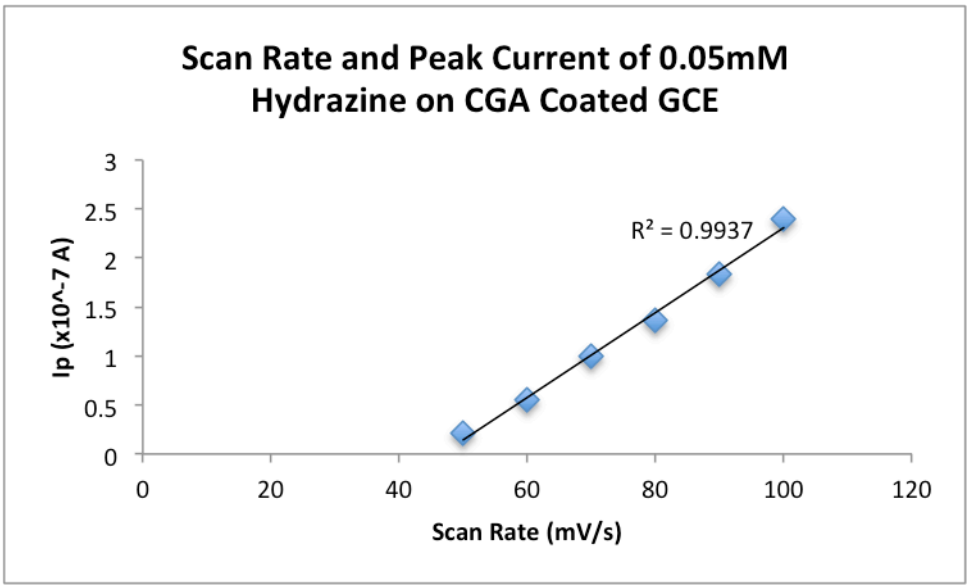

Figure 11. Scan Rate and Peak Current of 0.05mM Hydrazine on CGA Coated GCE in 0.15M PBS pH 7.5.

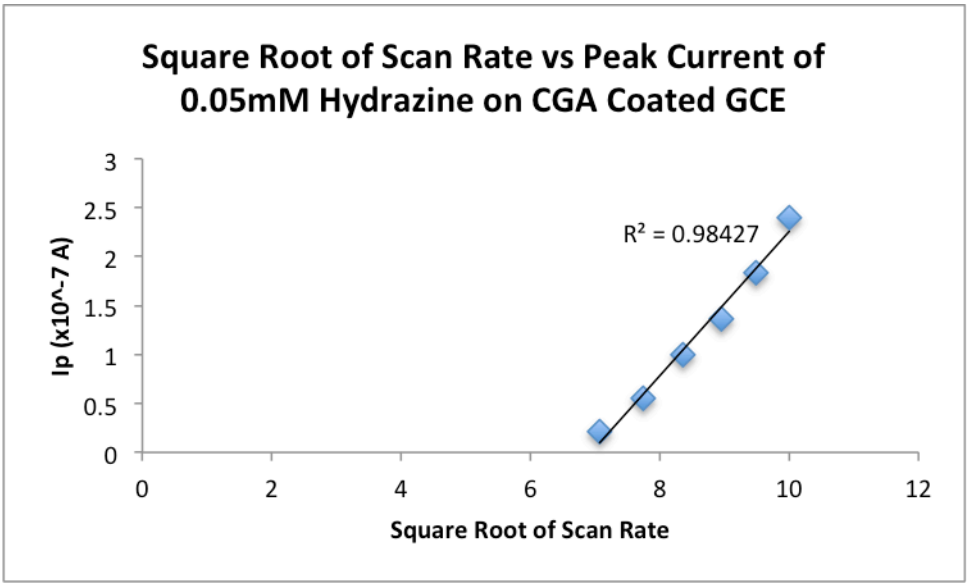

Figure 12. Square Root of Scan Rate and Peak Current of 0.05mM Hydrazine on CGA Coated GCE in 0.15M PBS pH 7.5.

Figure 12 gives change in current density with the square root of the scan rate. It shows that the peak current for the anodic oxidation of hydrazine is proportional to the square root of scan rate. This suggests that the catalytic oxidation of hydrazine in 0.15M PBS pH 7.5 involves mass transfer.

Our investigation is consistent with previous studies.[16a] A linear relationship in the plot of peak currents against the square root of the scan rates has been attributed to diffusion-controlled process.

4.1.1.3 Influence of pH. A study of the optimal pH for the catalytic oxidation of hydrazine at the CGA glassy carbon modified electrode in 0.15M PBS solution is shown in Figure 13 and tabulated in Table 3.

Table 3.

Concentration of Hydrazine on CGA Coated GCE at Each PBS pH.

Hydrazine Concentration (mM)	Ip_a ($x10^{-6}$ A)				
	pH 6	pH 7	pH 7.5	pH 8	pH 10
0.05	2.87	4.92	1.77	2.86	1.32
0.075	3.51	5.24	2.11	3.19	2.52
0.1	4.21	7.69	2.37	3.83	4.11
0.125	__	__	2.54	4.73	5.59
0.15	__	__	3.09	5.97	7.02
0.175	__	__	3.26	__	__

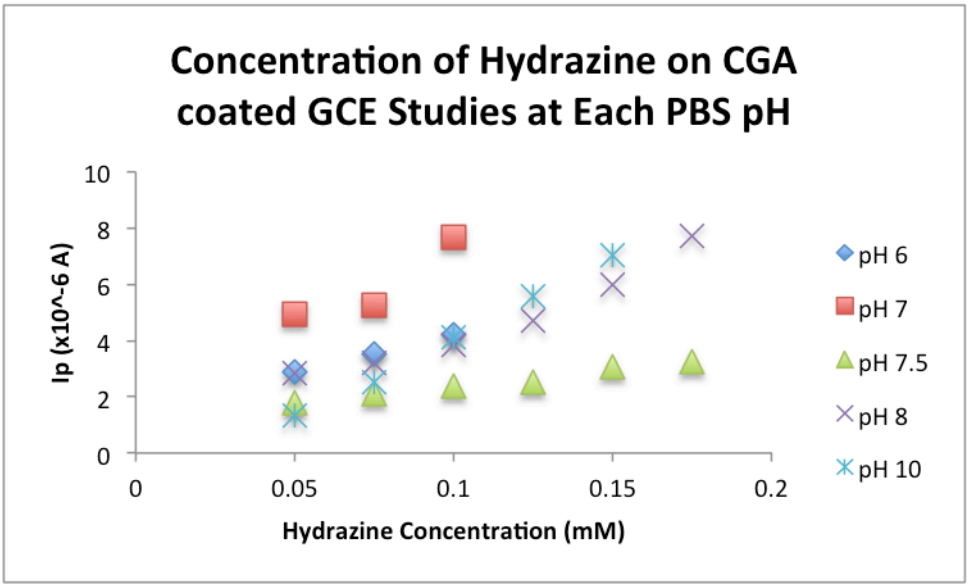

Figure 13. Concentration of hydrazine on CGA coated GCE at each pH in the range of pH 6-10 in 0.15M PBS solution at a scan rate of 25 mV/s.

It is shown from this study that increasing pH values from pH 6 to pH 7 increases the peak current at low hydrazine concentration. Results did not show proportionate increase at higher pH than 7. This cannot be explained. Results at pH 8 and pH 10 are also inconsistent. It therefore seems pH 7.5 is the optimal pH for performance of CGA on GCE.

4.1.1.4 Effect of Surfactant on the Electrode. The effect of surfactant on the electrode response to hydrazine on CGA modified GCE at 25mV/s in 0.15M PBS pH 7.5 is shown below in Table 4 and Figure 14. Each surfactant, SDS, DTAC, and DTAB, was tested independently.

Table 4.

Effect of Surfactant on CGA Coated GCE in 0.15M PBS pH 7.5 with 0.33 mM Hydrazine at 25 mV/s.

Concentration of Surfactant (µM)	Ip_a ($x10^{-6}$ A)		
	SDS	DTAC	DTAB
0.66	4.489	3.477	5.357
1.32	4.006	3.29	4.812
1.98	3.657	2.828	4.399
2.64	3.368	2.556	3.976
3.3	3.111	2.255	3.734
3.96	2.901	2.089	3.589
4.62	2.742	1.943	3.549
5.28	2.608	1.855	3.494

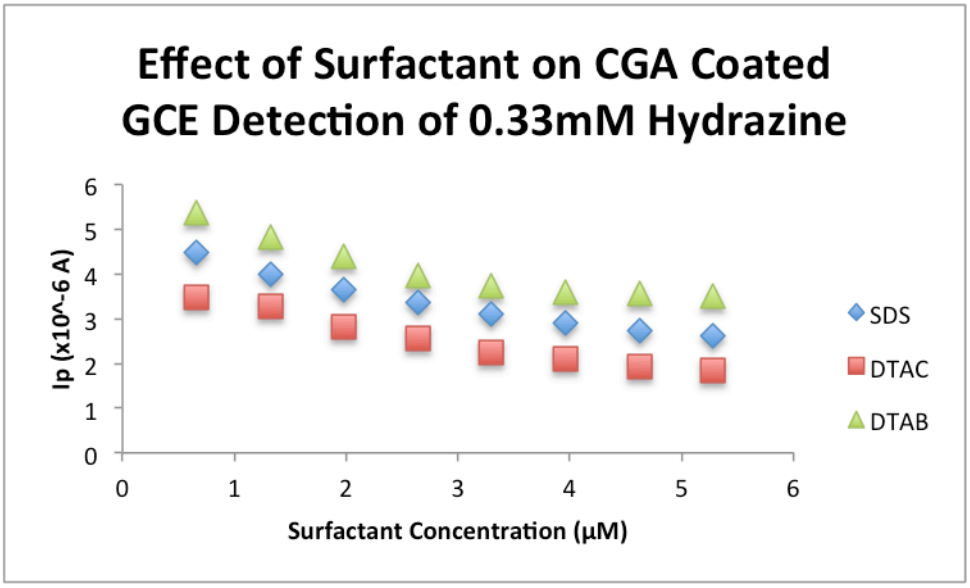

Figure 14. Effect of surfactant on CGA coated GCE detection of 0.33 mM hydrazine.

Studies[20] show that surfactants might affect electrochemical responses in two ways: structural or solubilizing. Table 6 shows that peak current decreases for various concentrations of surfactant. This indicates that neither structural nor solubilizing effect is evident in this study.

4.1.2 Detection of Nitrobenzene.

4.1.2.1 Nitrobenzene on Aspartic Acid Modified GCE. Glassy carbon electrode was coated with aspartic acid as described in Chapter 3. Cyclic voltammograms run before and after addition of nitrobenzene are shown in Figure 15.

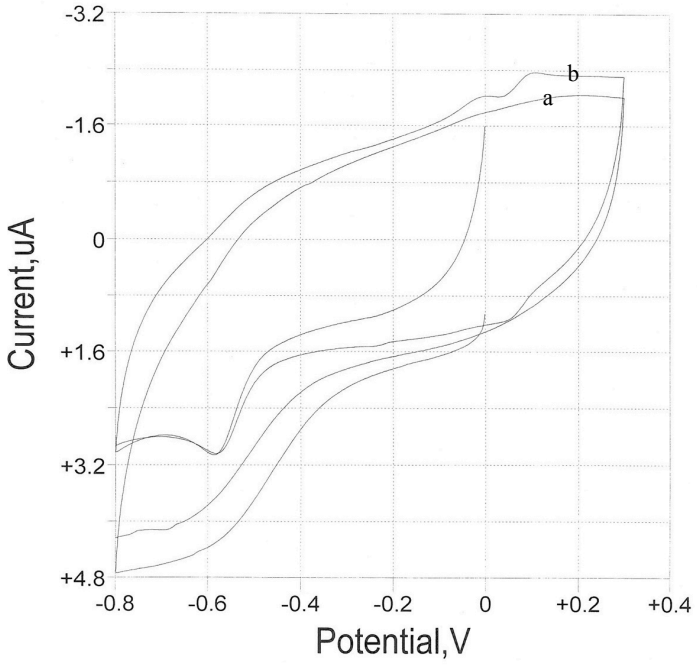

Figure 15. Cyclic voltammograms of an aspartic acid modified GCE at 25mv/s in 0.1M Acetic Acid Buffer pH 5.01. a) without nitrobenzene b) in the presence of 6.6µM nitrobenzene.

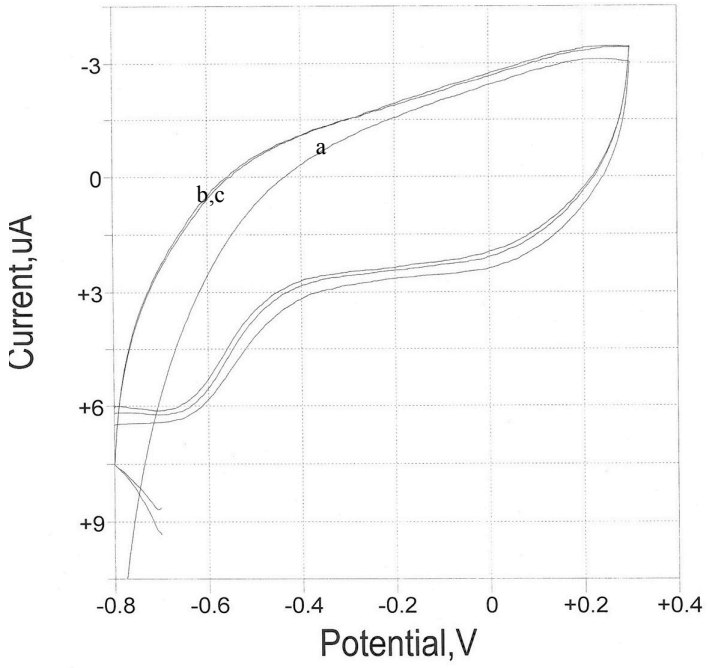

Figure 16. Cyclic voltammograms of a) bare GCE in 0.1M acetic acid buffer pH 5.02 b) bare GCE in 0.1M acetic acid buffer pH 5.01 with 3.3µM nitrobenzene c) bare GCE in 0.1M acetic acid buffer pH 5.01 with 1.3µM 4-nitrotoluene.

The cyclic voltammogram of nitrobenzene on aspartic acid modified GCE in 0.1 acetic acid buffer pH 5.01 is shown in Figure 15. The figure shows anodic peak current at about 0.105 mV at the modified electrode. There is a slight cathodic current observed at -0.583 mV. The peaks are separated by about 688 mV. Figure 16 shows there are no oxidation or reduction peaks in the voltammogram from presence of nitrobenzene at this lower concentration of 3.3µM.

4.1.2.1.1 Effect of Nitrobenzene Concentration. Figure 17 shows the cyclic voltammograms obtained for different concentrations of nitrobenzene.

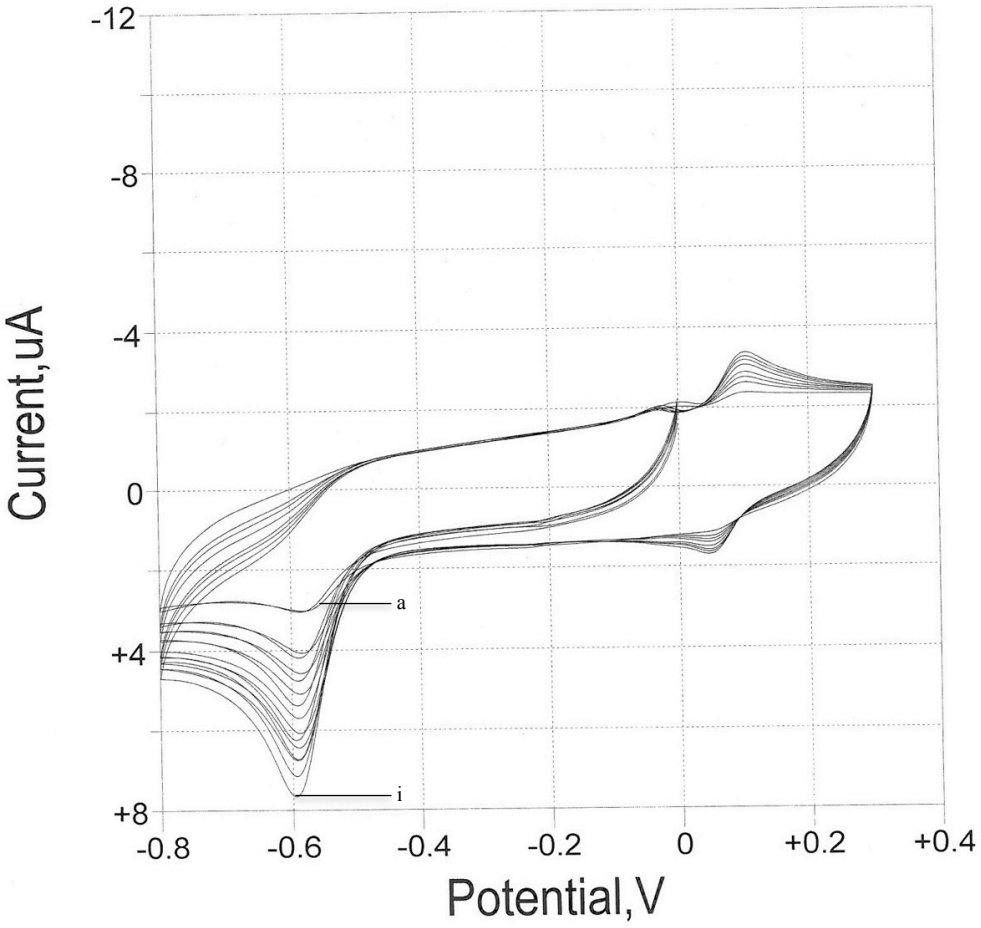

Figure 17. Cyclic voltammogram of aspartic acid modified electrode at 25mV/s in 0.1M acetic acid buffer pH 5.02.

The results from Figure 17 are tabulated in Table 5. The calibration curve constructed from the voltammograms of increasing nitrobenzene concentrations is shown in Figure 18.

Table 5.

Concentration of nitrobenzene on aspartic acid coated GCE and resulting peak currents as seen in Figure 17.

Concentration of Nitrobenzene (µM)	Ip_c (x10^-6 A)
(a) 6.6	1.24
(b) 9.9	1.88
(c) 13.2	2.33
(d) 16.5	2.86
(e) 19.8	3.37
(f) 23.1	4.03
(g) 26.4	4.42
(h) 29.7	4.78
(i) 33	5.11

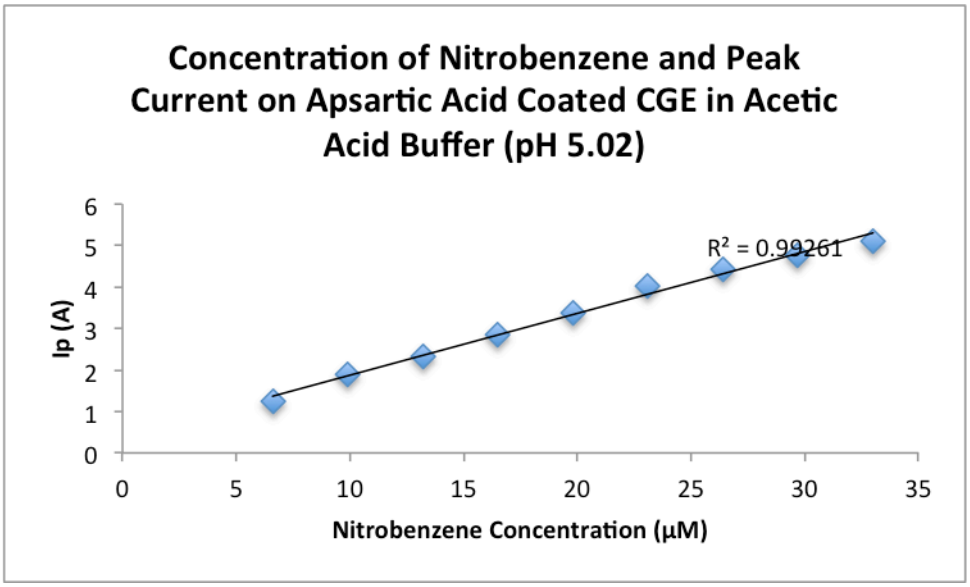

Figure 18. Concentration of nitrobenzene on aspartic acid coated GCE in 0.1M acetic acid buffer pH 5.02 at 25mV/s versus resulting peak current.

Observation from Figure 17 shows an anodic current at 105mV for each concentration from 6.6 µM to 33µM of nitrobenzene. No shift in the peak potential is visible from the result. However, the voltammograms show two cathodic peaks, one at 57mV and the other at -583mV

with a gradual shift towards the more negative. The calibration curve in Figure 18 shows a linear relationship between the current density and nitrobenzene concentration with a good linear regression curve with a correlation coefficient of 0.99261. The regression analysis with a low sensitivity of 6.6µM of nitrobenzene offer good precision and low detection limit with this method. This result shows good precision and technique for quantitative analysis of nitrobenzene.

4.1.2.1.2 Effect of Scan Rate. In Figure 19, the cyclic voltammograms of an aspartic acid coated GCE show the effect of current density at different scan rates. The scan rate against peak current is plotted in Figure 20. The peak current for the oxidation of nitrobenzene is plotted against the square root of the scan rate and represented in Table 8 and Figure 21.

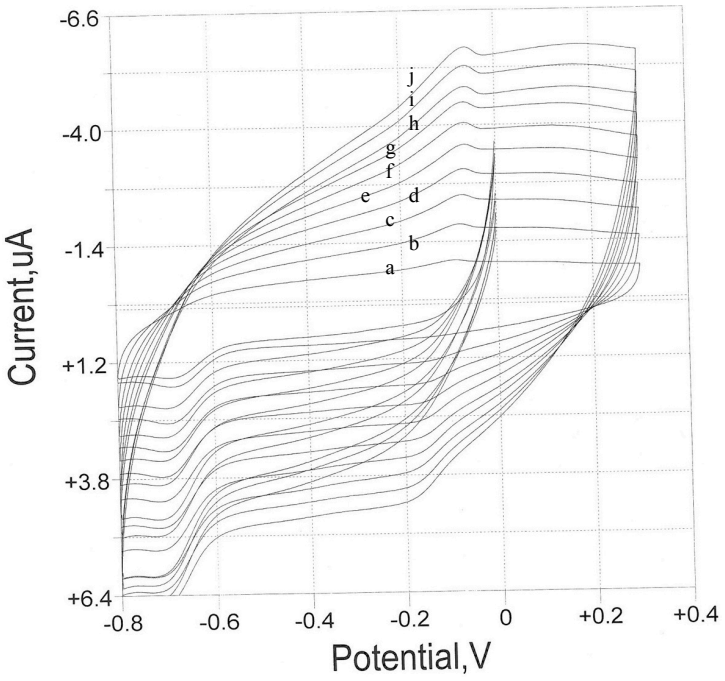

Figure 19. Cyclic voltammograms of aspartic acid modified GCE at various scan rates in 0.1M acetic acid buffer pH 5.02 with 3.3 µM nitrobenzene. Scan rates are a) 10, b) 20, c) 30, d) 40, e) 50, f) 60, g) 70, h) 80, i) 90, and j) 100.

Table 6.

Scan Rate, Square Root of Scan Rate and Peak Current of 3.3 µM Nitrobenzene on Aspartic Acid Coated GCE

Scan Rate (mV/s)	Square Root of Scan Rate	Ip_c (x10^-6 A)
(a) 10	3.2	0.785
(b) 20	4.5	0.99
(c) 30	5.5	1.08
(d) 40	6.3	1.17
(e) 50	7.1	1.24
(f) 60	7.7	1.35
(g) 70	8.4	1.38
(h) 80	8.9	1.53
(i) 90	9.5	1.56
(j) 100	10	1.61

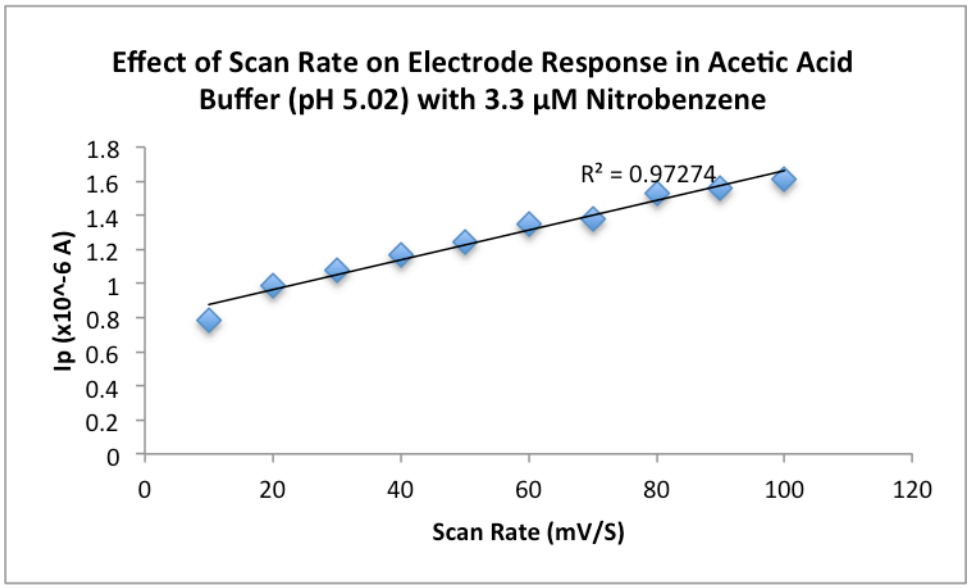

Figure 20. Scan Rate against Peak Current of 3.3 µM Nitrobenzene on Aspartic Acid Coated GCE in 0.1M acetic acid buffer pH 5.02.

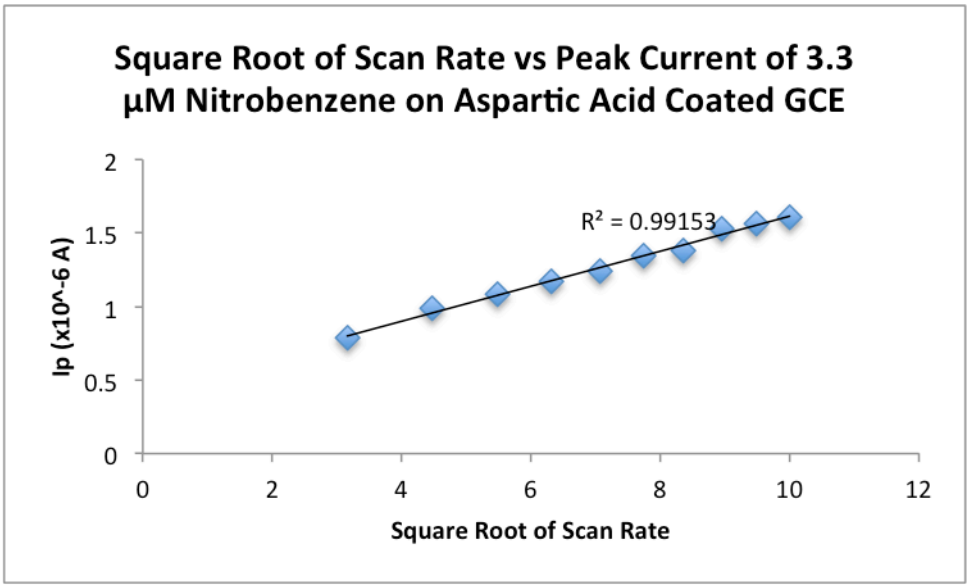

Figure 21. Square Root of Scan Rate against Peak Current 3.3 µM Nitrobenzene on Aspartic Acid Coated GCE in 0.1M acetic acid buffer pH 5.02.

The linear plots in Figures 20 and 21 for 3.3 µM of nitrobenzene show linear regression curves with correlation coefficients of 0.97274 and 0.99153, respectively. These results imply that the electro-reduction and electro-oxidation was most probably a diffusion-controlled process. Similar plots were obtained for aspartic acid coated GCE for nitrotoluene by earlier investigators.[16c, 18] The diffusion controlled process is further affirmed by the result of plotting the current density against the square root of the scan rate, shown in Figure 21, resulting in a linear curve.

4.1.2.1.3 Influence of pH. Table 7 and Figure 22 shows the effect of pH on the electrocatalytic oxidation of nitrobenzene on aspartic acid modified GCE.

Table 7.

Concentration of Nitrobenzene on Aspartic Acid Coated GCE at Each Acetic Acid Buffer pH.

Concentration of Nitrobenzene (µM)	Ip_c (x10^-6 A)				
	pH 2.41	pH 4.01	pH 5.02	pH 6.84	pH 8.03
6.6	1.84	1.23	1.24	0.784	1.01
9.9	2.14	1.71	1.88	1.11	1.4
13.2	2.45	1.93	2.33	1.46	1.68
16.5	2.79	2.06	2.86	1.61	1.94
19.8	3.45	2.40	3.37	2.01	2.09
23.1	3.9	2.81	4.03	2.26	2.17
26.4	4.46	3.31	4.42	2.58	2.45
29.7	5.11	3.69	4.78	2.8	2.6

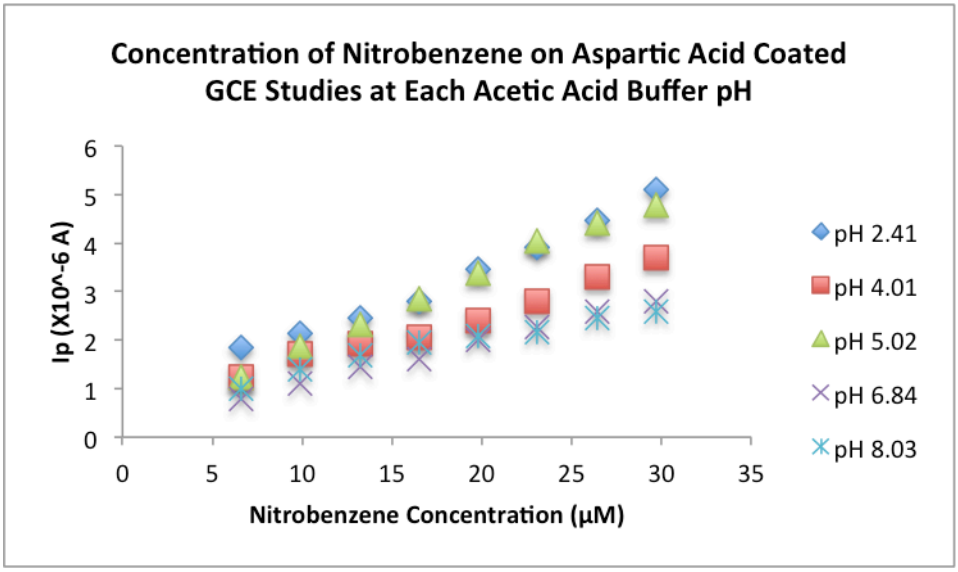

Figure 22. Concentration of Nitrobenzene on Aspartic Acid Coated GCE at Each Acetic Acid Buffer pH.

Table 10 shows that at each pH, cathodic reduction of nitrobenzene increases with the concentration of the substrate. However, the relationship, as shown in Figure 22, is not regular

linear trend. This irregularity is also depicted on Table 7. The erratic results make it difficult to assign the pH of optimum electrode reaction.

4.1.2.1.4 Effect of Surfactant. Effect of surfactant on the electrode response to nitrobenzene on aspartic acid GCE at a scan rate of 25mV/s in 0.1M acetic acid buffer pH 5.02 is shown below in Table 8 and Figure 23.

Table 8.

Effect of Surfactant on Aspartic Acid Coated GCE Detection of 0.33 mM Nitrobenzene.

Concentration of Surfactant (µM)	Ip_c (x10^-6 A)		
	SDS	DTAC	DTAB
0.66	0.474	0.436	0.438
1.32	0.564	0.42	0.428
1.98	0.629		0.408
2.64	0.707		0.396
3.3	0.766		0.423
3.96	0.757		0.424
4.62	0.751		0.414
5.28	0.699		0.429

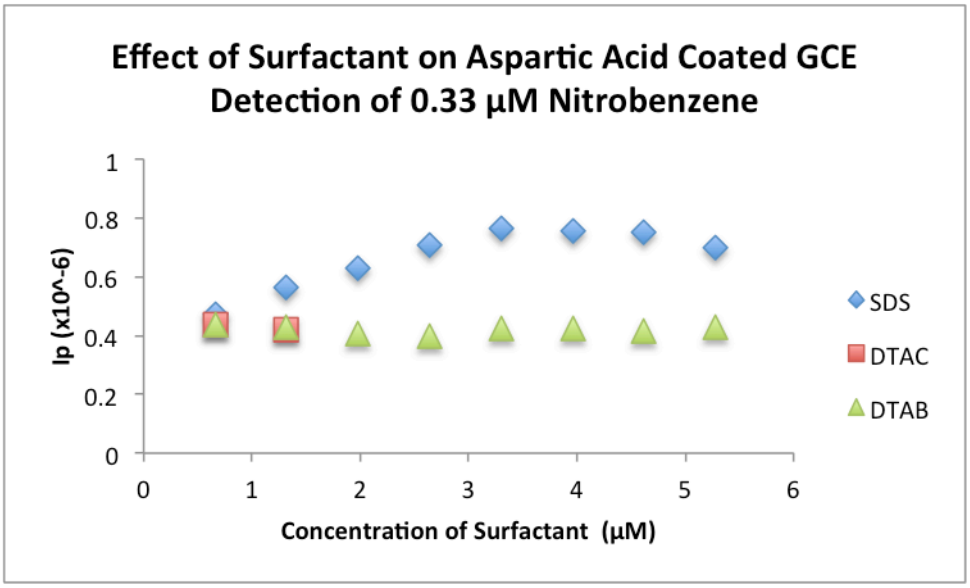

Figure 23. Effect of Surfactant on Aspartic Acid Coated GCE Detection of 0.33 mM Nitrobenzene.

On Table 8, there is a gradual increase in peak current of nitrobenzene on aspartic acid coated GCE in acetic acid buffer pH 5.02 as the SDS concentration increases. The opposite is true for DTAC and DTAB. This molecular structure of SDS probably makes it easier than those of DTAC and DTAB to absorb onto the hydrophobic surface of the GCE.

The results are shown in Figure 23 where DTAB changes minimally the current density over a concentration range of 0.66 µM to 5.28 µM of DTAB whereas electrode response to the addition of SDS show slight increase up to about 4 µM of the surfactant. This increase, however, is not significant to cause an enhancement of the electrocatlytic oxidation of nitrobenzene on aspartic acid coated GCE.

4.1.2.2 Nitrobenzene on Phenol Red Coated GCE. Glassy carbon electrode was coated with phenol red as described in Chapter 3. Cyclic voltammograms run before and after the addition of nitrobenzene are shown in Figure 24.

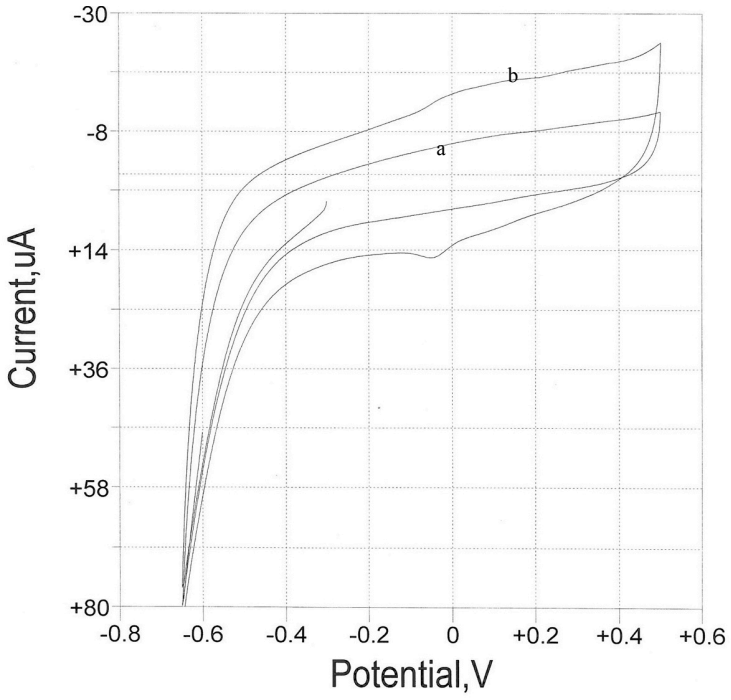

Figure 24. Cyclic voltammogram of a phenol red modified GCE at 100mV/s in 0.15M PBS pH 7.5, a) without nitrobenzene, b) with 3.3µM nitrobenzene.

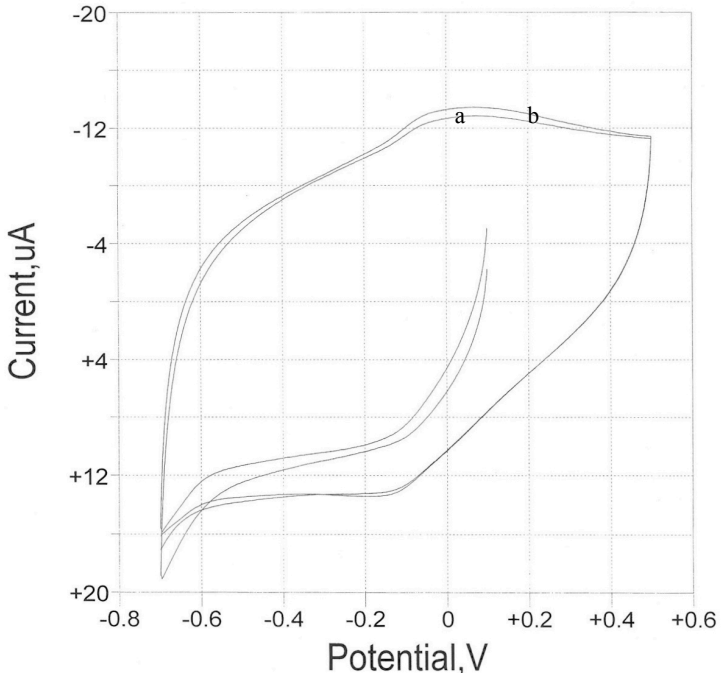

Figure 25. Cyclic voltammograms of a) bare GCE in 0.15M PBS pH 7.5 b) bare GCE in 0.15M PBS pH 7.5 with 3.3µM nitrobenzene.

As shown in Figure 24, there is only a reduction point at -42mV. In Figure 25, there are no oxidation or reduction peaks in either voltammogram of the uncoated electrode.

4.1.2.2.1 Effect of Nitrobenzene Concentration. Figure 26 shows the cyclic voltammograms obtained for different concentrations of nitrobenzene. The calibration curve constructed from the voltammograms is represented in Table 9 and Figure 27.

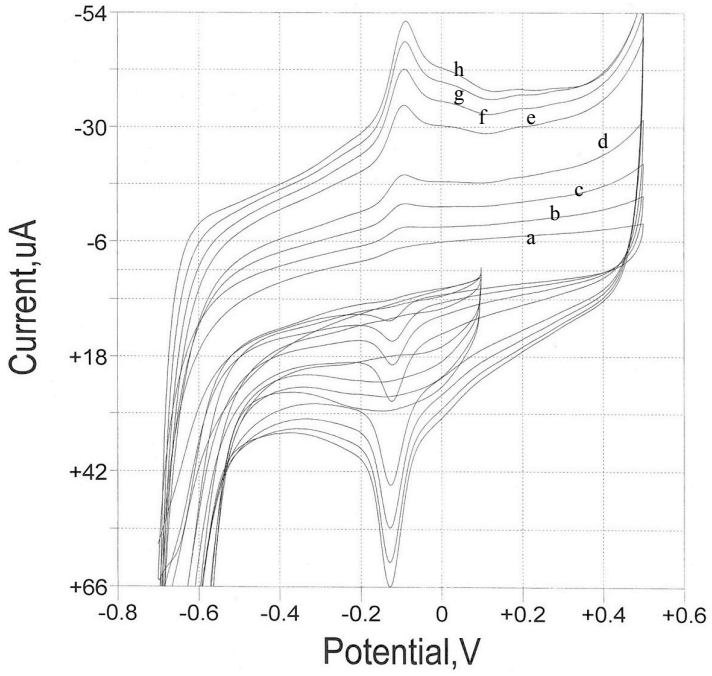

Figure 26. Cyclic voltammogram response of phenol red modified GCE at 100mV/s in 0.15M PBS pH 6.0. Nitrobenzene concentrations are detailed in Table 13.

Table 9.

Concentration of Nitrobenzene on Phenol Red Coated CGE

Nitrobenzene Concentration (µM)	Ip_c (x10^-6 A)
3.3	2.49
6.6	5.62
9.9	8.74
13.2	10.4
16.5	12.9
19.8	16.2
23.1	18.4
26.4	19.6

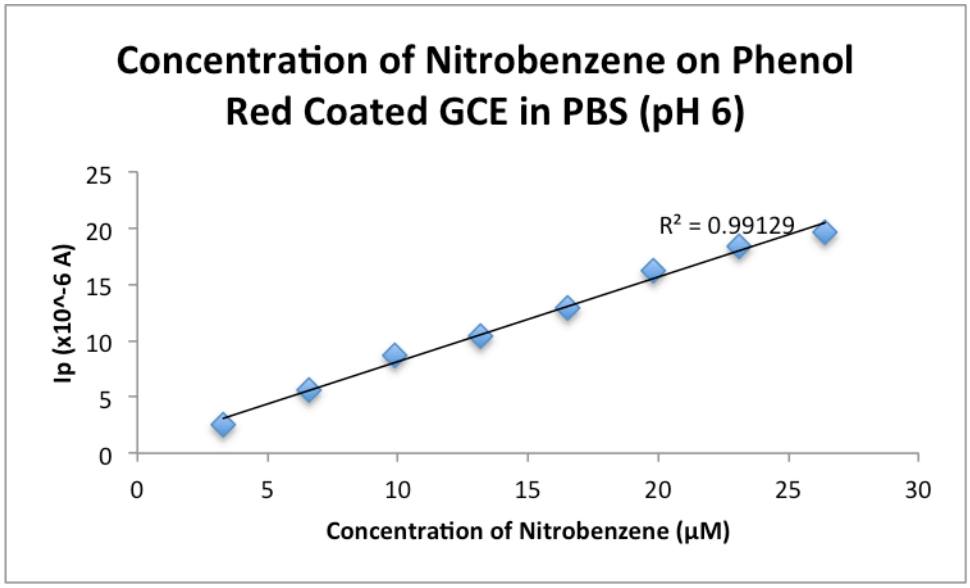

Figure 27. Concentration of Nitrobenzene on Phenol Red Coated GCE.

The cyclic voltammogram in Figure 26 clearly shows that the reduction peak currents at -160 mV increase progressively as the concentration of nitrobenzene increases. The same trend is observed in the peak currents for oxidation at about 150 mV. A correlation coefficient of 0.99129 of the cathodic peak current shown in Figure 27 indicates a sensitive electrode response to the nitrobenzene detection and quantitative analysis. To the best of our knowledge this poly (phenol red) coated GCE has been used for trace determination of Lead (II) by differential pulse anodic stripping voltammetry.[19] However the use of this kind of modified electrode to detect or quantify nitrobenzene is not found in literature. We ascertain that this is the first time that behavior of nitrobenzene at poly (phenol red) modified GCE is investigate.

4.1.2.2.2 Effect of Scan Rate. In Figure 28, the cyclic voltammograms of an aspartic acid coated GCE show the effect of current density at different scan rates. The peak current for the oxidation of nitrobenzene is plotted against the square root of the scan rate and represented in Table 10 and Figure 29.

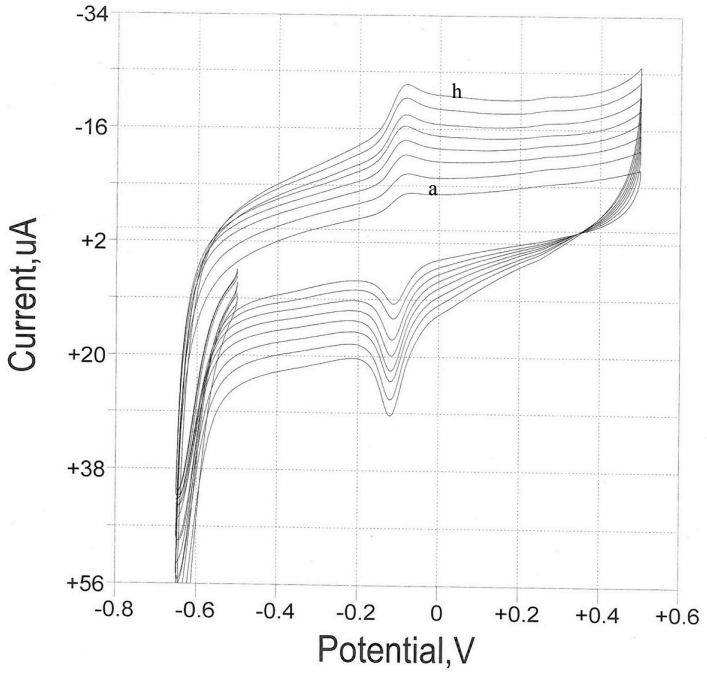

Figure 28. Cyclic voltammogram of phenol red modified GCE at various scan rates in 0.15M PBS pH 6. Scan rates are (a) 60, 70, 80, 90, 100, 110, 120 and (h) 130 mV/s.

Table 10.

Scan Rate, Square Root of Scan Rate and Peak Current of 3.3 µM Nitrobenzene on Phenol Red Coated GCE in 0.15M PBS pH 6.

Scan Rate (mV/s)	Square Root of Scan Rate	Ip_c (x10^-6 A)
(a) 60	7.7	5.923
(b) 70	8.4	6.863
(c) 80	8.9	8.732
(d) 90	9.5	9.882
(e) 100	10	10.75
(f) 110	10.5	10.73
(g) 120	11.0	11.84
(h) 130	11.4	12.06

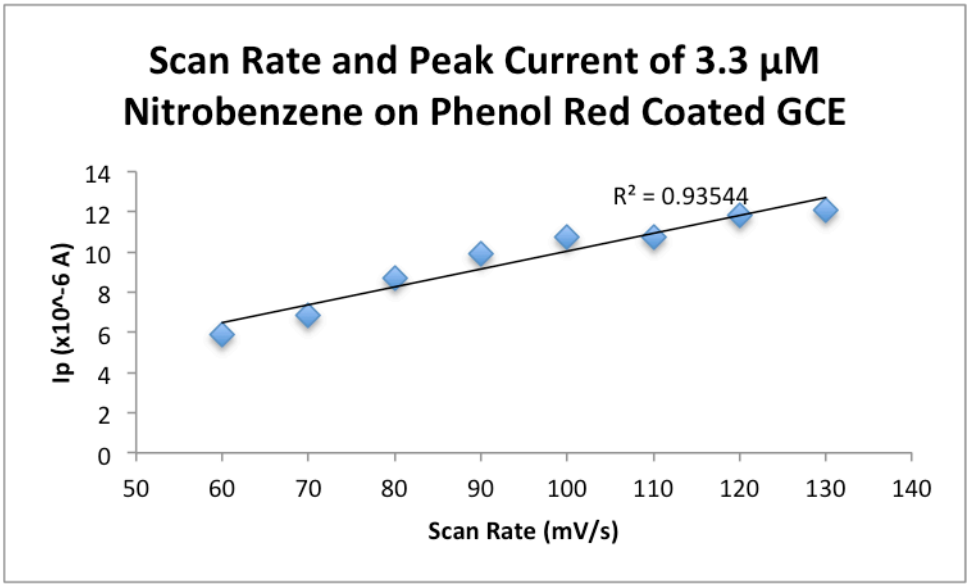

Figure 29. Scan Rate and Peak Current of 3.3 µM Nitrobenzene on Phenol Red Coated GCE in 0.15M PBS pH 6.

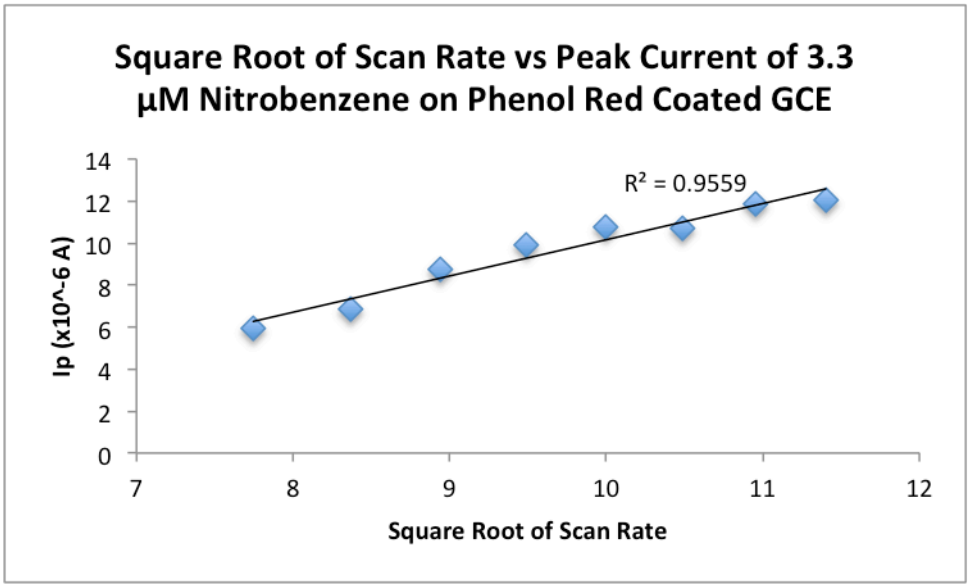

Figure 30. Square Root of Scan Rate and Peak Current of 3.3 µM Nitrobenzene on Phenol Red Coated GCE in 0.15M PBS pH 6.

A linear relationship in the plot of peak currents against the square root of the scan rates has been attributed to a diffusion-controlled process.

4.1.2.2.3 Influence of pH. Table 11 and Figure 31 show the effect of pH on the electrocatalytic oxidation of nitrobenzene on phenol red coated GCE.

Table 11.

Concentration of Nitrobenzene on Phenol Red Coated GCE at Each PBS pH.

Concentration of Nitrobenzene (µM)	Ip_c (x10^{-6} A)					
	pH 4	pH 5	pH 6	pH 7.5	pH 8	pH 10
3.30	3.04	3.28	2.49			
5.00				4.07		
6.60	5.44	6.23	5.62		2.60	
9.90	6.23	9.56	8.74		4.72	
10.00				6.68		
13.20	8.00	13.00	10.40		6.16	
15.00				8.75		2.7
16.50	10.20	17.40	12.90		7.48	
19.80	6.49	20.10	16.20		10.00	
20.00				12.10		3.69
23.10	13.00	18.90	18.40		12.50	
25.00				18.70		4.99
26.40	12.60	23.80	19.60		13.40	
30.00				23.40		4.82
35.00				27.00		5.65
40.00				29.70		6.50

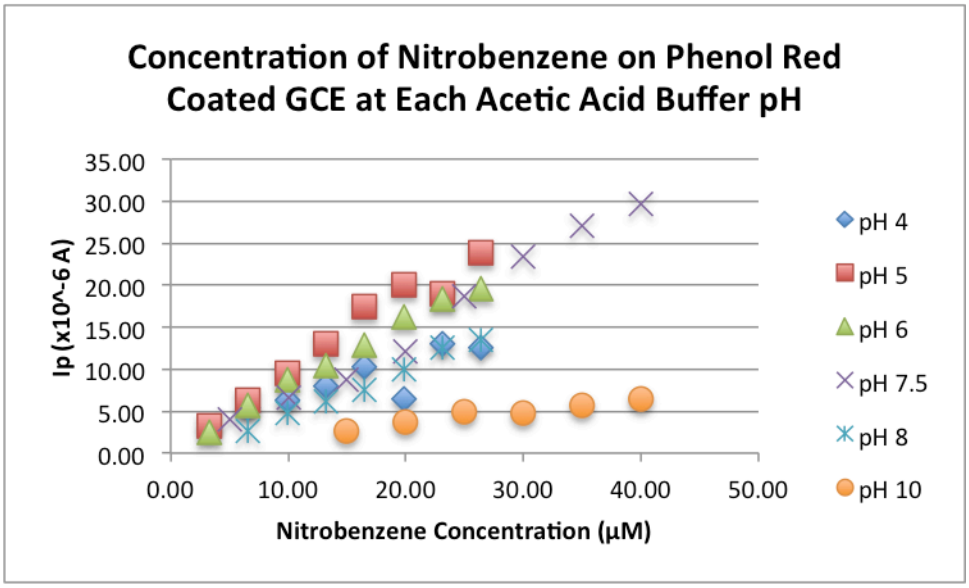

Figure 31. Concentration of Nitrobenzene on Phenol Red Coated GCE at Each PBS pH.

A study of the optimal pH for the catalytic oxidation and reduction of nitrobenzene at the phenol red modified GCE in 0.15M PBS in the pH range 4-10 is tabulated on Table 11 and Figure 31. The study shows that at low pHs 4 and 5, cathodic current density increases with increasing concentration. This increase is more conspicuous at pH of 5. The highest peak current of 3.28x10-6 A was obtained for 3.3 µM nitrobenzene.

At any specific concentration increase in current density is also more obvious at pHs 4 and 5 than at higher pHs. It shows that pH 5 give optimum results. At basic pHs, such as 8 an 10, current density on phenol red modified electrode is considerably minimized.

Table 11 also shows that at high nitrobenzene concentrations (30-40 µM) the electrode response is visible at pH 7.5, where such a response is not observed at pH 4-6. In general, the phenol red modified GCE is more sensitive to the detection of nitrobenzene at acidic pH (4-6) than basic pH (8-10).

4.1.2.2.4 Effect of Surfactant. The effect of surfactant on the electrode response to nitrobenzene on phenol red coated GCE at a scan rate 100mV/s in 0.15M PBS pH 6 is shown below in Table 12 and Figure 32.

Table 12.

Effect of Surfactant on Phenol Red Coated GCE Detection of 0.33mM Nitrobenzene.

Concentration of Surfactant (µM)	Ip_c ($x10^{-6}$ A)		
	SDS	DTAC	DTAB
0.66	7.369	6.6	3.589
1.32	7.142	5.315	3.195
1.98	6.276	3.319	3.348
2.64	6.421	1.96	1.961
3.3	5.549	1.502	2.073
3.96	5.837	1.754	2.088
4.62	5.745	1.814	1.889
5.28	5.648	1.396	2.015

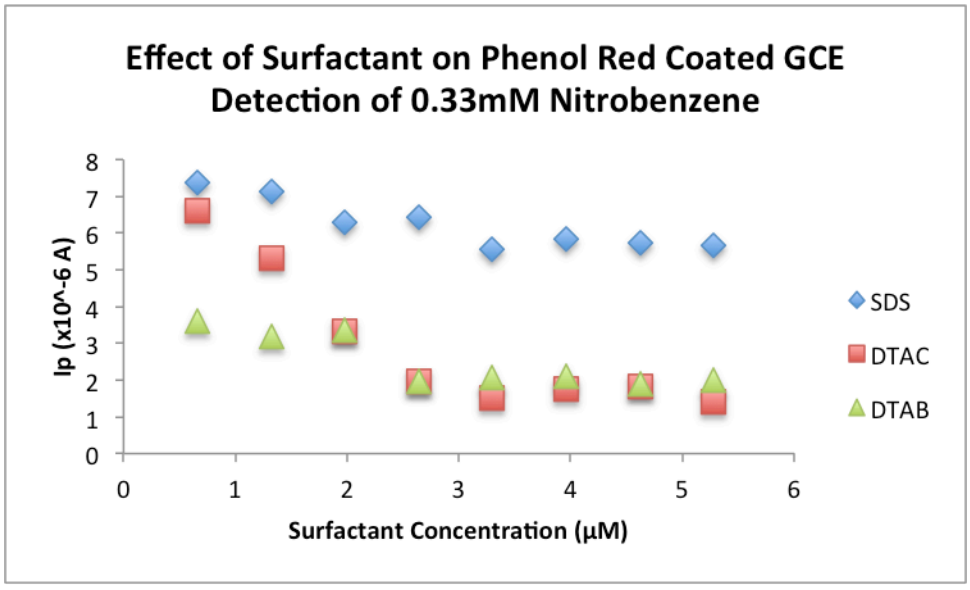

Figure 32. Effect of Surfactant on Phenol Red GCE Detection of 0.33mM Nitrobenzene in 0.15M PBS pH 6 at scan rate 100 mV/s.

The addition of surfactant to the electrochemical cell resulted a decrease in the peak current as increasing concentrations of each surfactant. Both DTAB and SDS caused a gradual decrease, while DTAC caused a sudden decrease until 2.64 μM then a more gradual decrease.

Studies[20] show that surfactants could enhance electrochemical responses primarily by solubilization. All three of the surfactants studied here did not enhance, but instead caused an interruption in the performance of the electrode.

4.1.3 4-Nitrotoluene on Modified GCE. Glassy carbon electrode was modified with aspartic acid as described in Chapter 3. Cyclic voltammograms run before and after the addition of 4-nitrotoluene is shown in Figure 33.

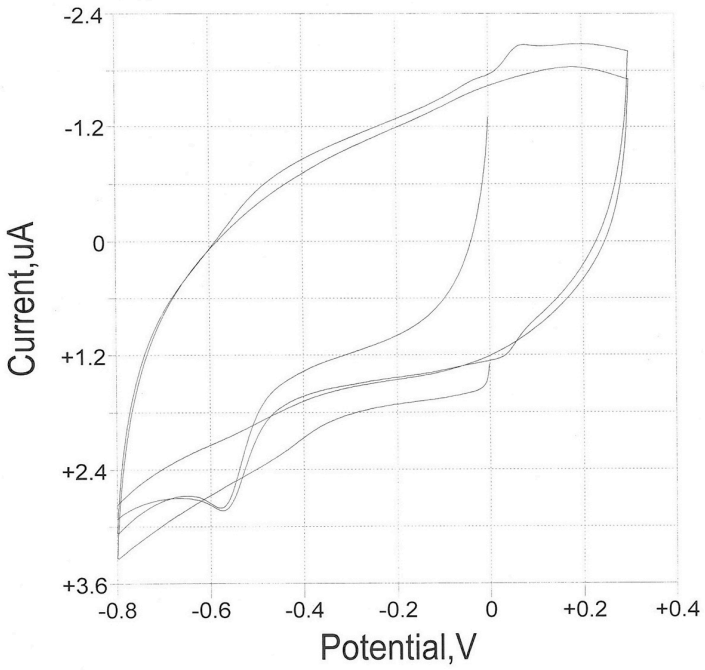

Figure 33. Cyclic voltammograms of aspartic acid coated GCE at 25mV/s in 0.1M acetic acid buffer pH 5.02.

As shown in Figure 33, the two peaks showing catalytic reduction (-573mV) and slight oxidation current (65mV), both of which are separated by about 638mV. Figure 16 shows the

uncoated GCE with and without 4-nitrotoluene. There are no oxidation or reduction peaks for these voltammograms.

4.1.3.1 Effect of 4-Nitrotoluene Concentration. In Figure 34, the cyclic voltammograms obtained for different concentrations of 4-nitrotoluene are shown. The calibration curve constructed from the voltammograms is shown on Table 13 and Figure 35.

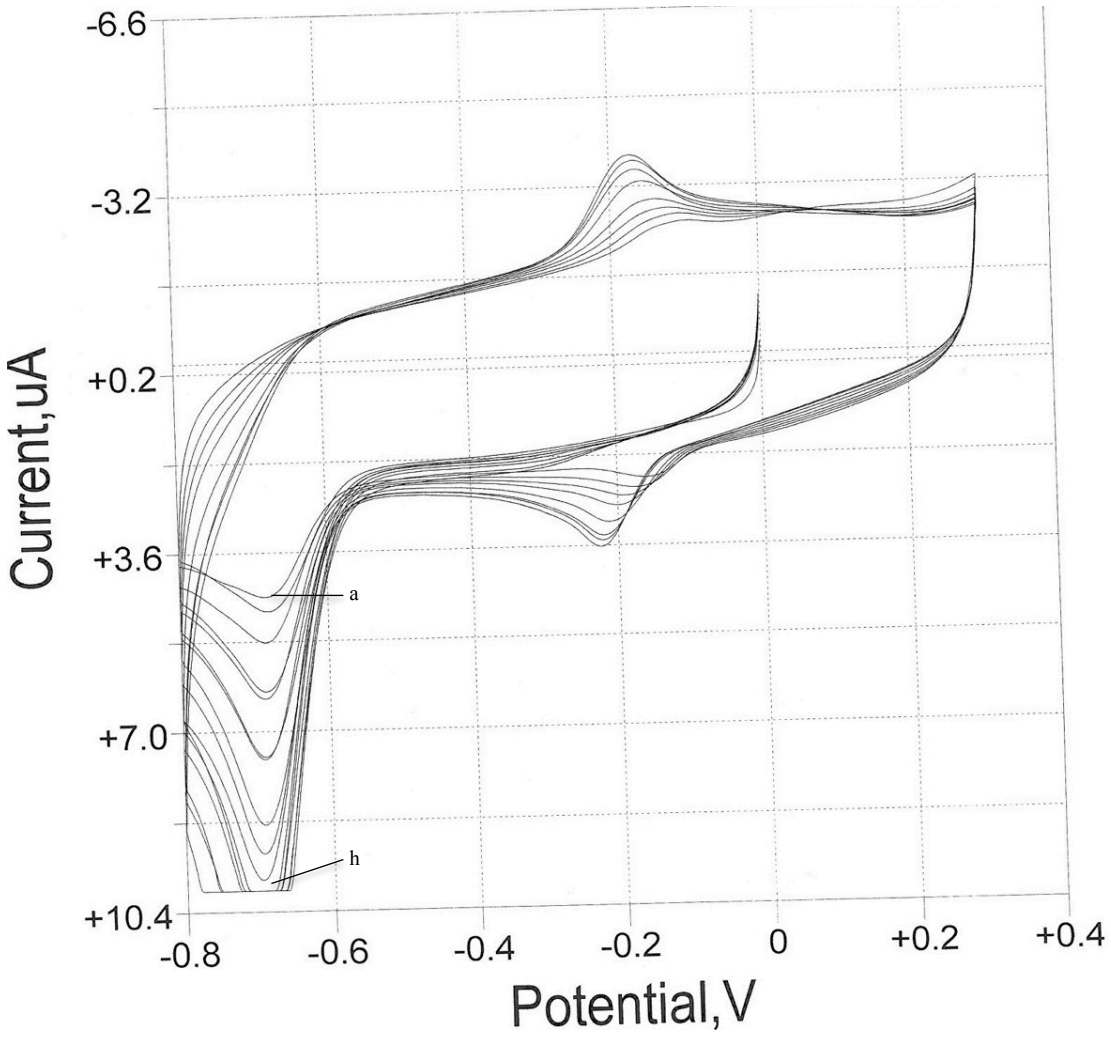

Figure 34. Cyclic voltammogram response of an aspartic acid coated GCE at 25mV/s in 0.1 acetic acid buffer pH 5.02. 4-nitrotoluene concentrations are tabulated in Table 13.

Table 13.

Concentration of 4-nitrotoluene on aspartic acid coated GCE and peak current.

Concentration of 4-Nitrotoluene (µM)	Ip_c ($x10^{-6}$ A)
(a) 1.3	1.08
(b) 2.6	2.38
(c) 3.9	3.4
(d) 5.2	4.58
(e) 6.5	5.38
(f) 7.8	6.15
(g) 9.1	7.48
(h) 10.4	8.38

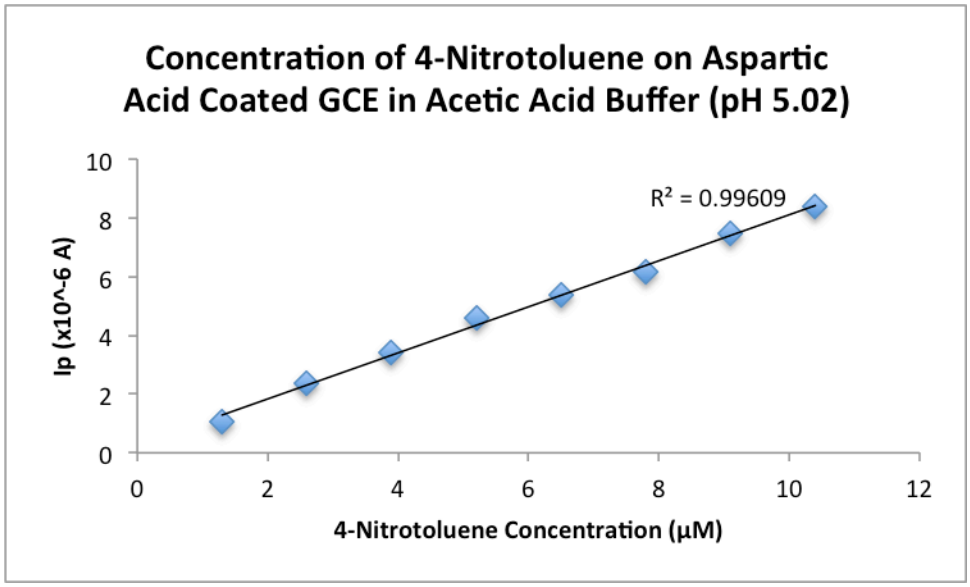

Figure 35. Concentration of 4-nitrotoluene on aspartic acid coated GCE in 0.1 acetic acid buffer pH 5.02 at scan rate 25 mV/s.

The linear correlation of 0.99609 suggests that this method could be used for both qualitative and quantitative detection of 4-nitrotoluene.

4.1.3.2 Effect of Scan Rate. In Figure 36, the cyclic voltammograms of an aspartic acid coated GCE show the effect of current density at different scan rates. The peak current for the oxidation of nitrobenzene is plotted against the scan rate in figure 37, and against the square root of the scan rate in Figure 38. All data from this study are tabulated in Table 14.

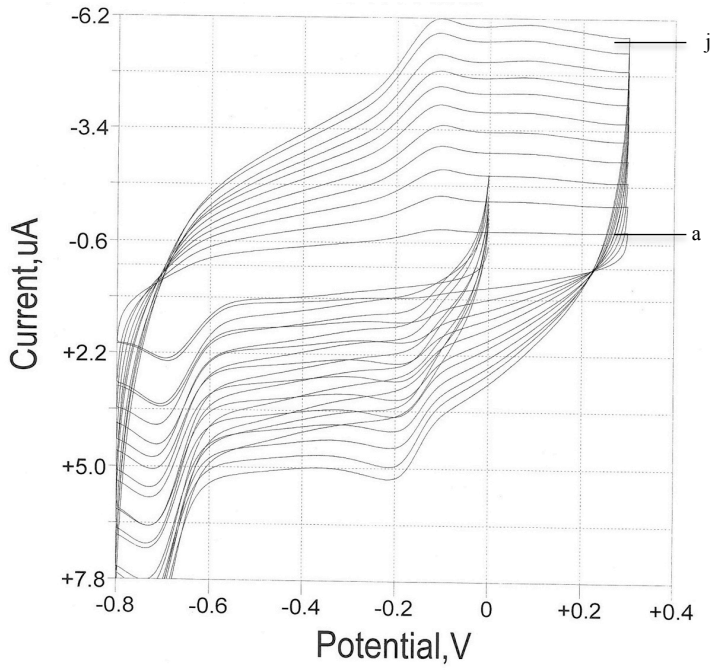

Figure 36. Cyclic voltammogram of aspartic acid modified GCE at various scan rates in 0.1M acetic acid buffer pH 5.02. Scan rates are detailed in Table 19.

Table 14.

Scan rate, square root of scan rate and peak current of 1.3 µM 4-nitrotoluene on aspartic acid coated GCE in 0.1M acetic acid buffer pH 5.02.

Scan Rate (mV/s)	Square Root of Scan Rate	Ip_c ($x10^{-6}$ A)
(a) 10	3.2	1.39
(b) 20	4.5	1.84
(c) 30	5.5	2.19
(d) 40	6.3	2.36
(e) 50	7.1	2.58
(f) 60	7.7	2.89
(g) 70	8.4	3.04
(h) 80	8.9	3.41
(i) 90	9.5	3.69
(j) 100	10.	3.67

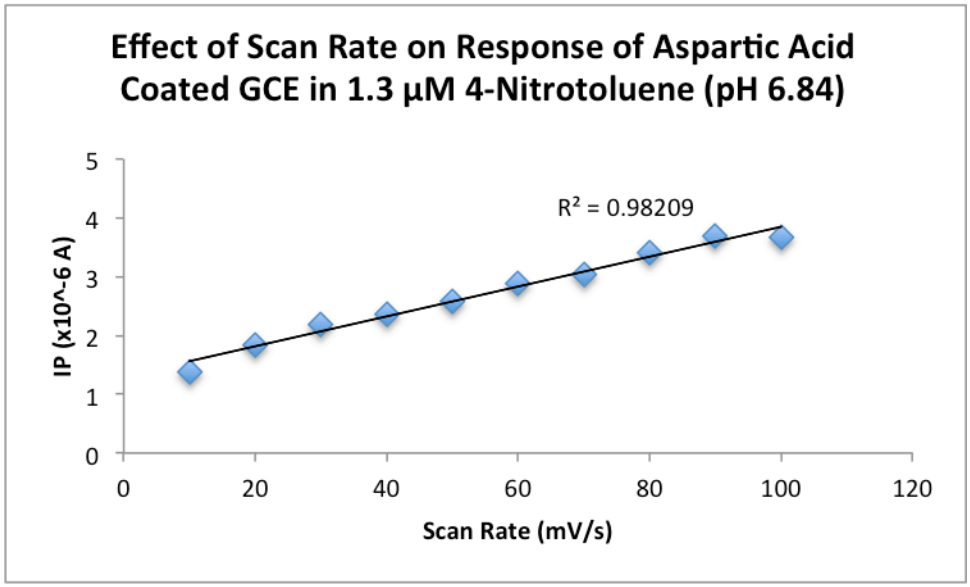

Figure 37. Scan rate and peak current of 1.3 µM 4-nitrotoluene on aspartic acid coated GCE in 0.1M acetic acid buffer pH 5.02.

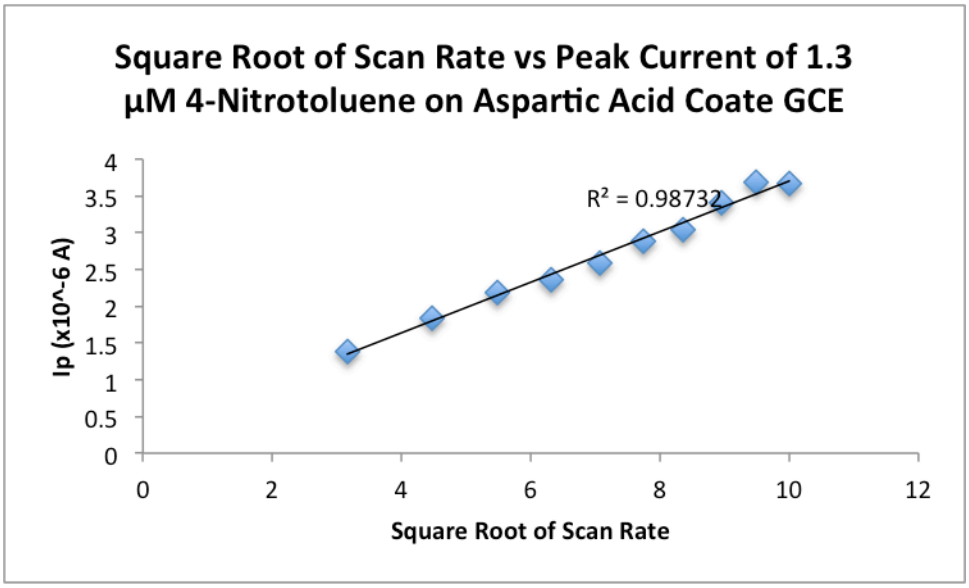

Figure 38. Square root of scan rate and peak current of 1.3 µM 4-nitrotoluene on aspartic acid coated GCE in 0.1M acetic acid buffer pH 5.02.

A linear relationship in the plot of peak currents against the square root of the scan rates has been attributed to a diffusion-controlled process.

4.1.3.3 Influence of pH. Table 15 and Figure 39 shows the effect of pH on the electrocatalytic oxidation of 4-nitrotoluene on aspartic acid modified GCE.

As seen in table 15, the electrode was unable to detect concentrations above 6.5 µM at pH 10. Figure 39 shows the plot of the 4-nitrotoluene concentrations against peak current. At pH 5.02, the highest correlation coefficient of 0.99609 was observed indicating that this pH provided the most stability. At pH 4.01, the peak current was highest for 1.3 µM 4-nitrotoluene showing the highest sensitivity at this pH.

Table 15.

Concentration of 4-nitrotoluene on aspartic acid coated GCE at each pH in acetic acid buffer pH.

Concentration of 4-Nitrotoluene (µM)	Ip_c ($x10^{-6}$ A)					
	pH 2.41	pH 4.01	pH 5.02	pH 6.84	pH 8.03	pH 10
1.3	0.0809	1.3	1.08	1.4	0.897	1.45
2.6	0.177	2.45	2.38	2.37	2.52	2.32
3.9	0.276	3.37	3.4	3.2	3.03	4.42
5.2	0.397	4.57	4.58	3.82	3.76	6.98
6.5	0.512	5.54	5.38	4.48	5.05	8.04
7.8	0.802	6.26	6.15	5.02	5.94	
9.1	0.925	7.14	7.48	5.35	6.46	
10.4	0.988	7.99	8.38	5.81	7.11	

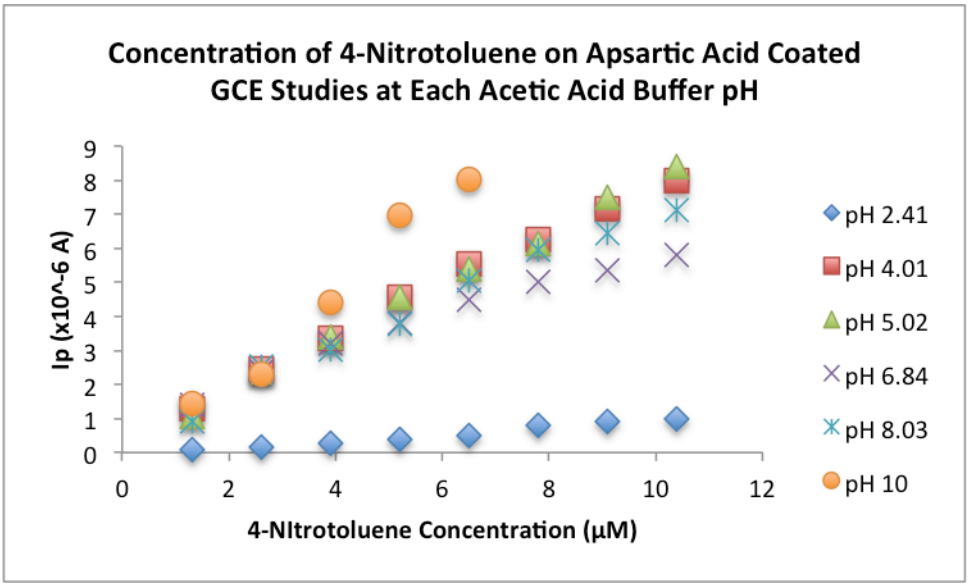

Figure 39. Concentration of 4-Nitrotoluene on Aspartic Acid Coated GCE at Each Acetic Acid Buffer pH.

4.1.3.4 Effect of Surfactant. The effect of surfactant on the electrode response to 4-nitrotoluene on aspartic acid modified GCE at 25mV/s in 0.1M acetic acid buffer pH 5.02 is shown in Table 16 and Figure 40.

Table 16.

Effect of Surfactant on Aspartic Acid Coated GCE Detection of 1mM 4-Nitrotoluene.

Concentration of Surfactant (µM)	Ip_c ($x10^{-6}$ A)		
	SDS	DTAC	DTAB
0.66	4.35	4.31	3.89
1.32	3.16	4.26	3.61
1.98	3.62	4.11	3.47
2.64	3.99	4.08	3.21
3.3	2.85	4.04	3.04
3.96	2.65	3.55	2.77
4.62	4.56	3.95	2.71
5.28	1.63	3.92	2.63

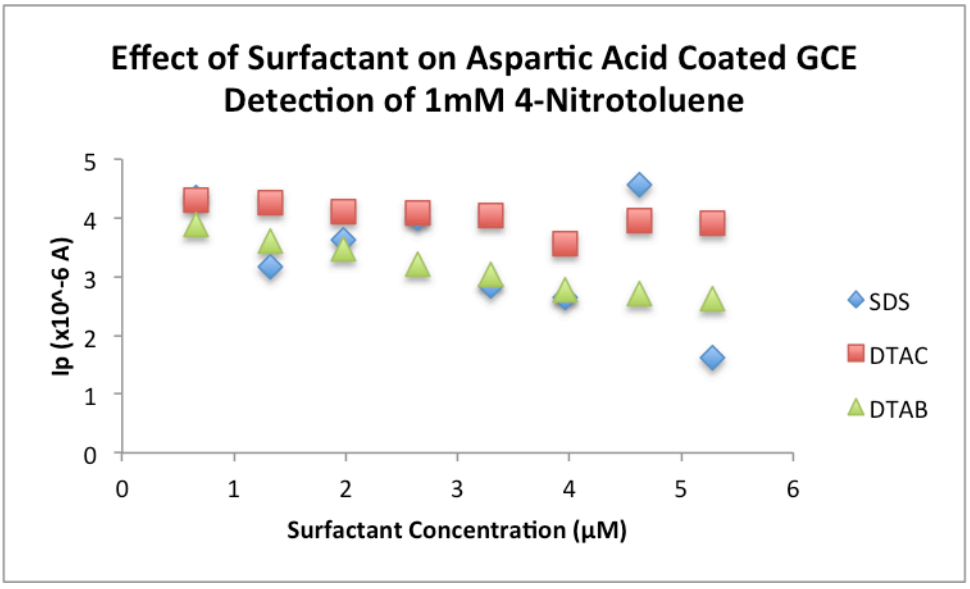

Figure 40. Effect of Surfactant on Aspartic Acid Coated GCE Detection of 1mM 4-Nitrotoluene in 0.1M acetic acid buffer pH 5.02 at scan rate 25 mV/s.

The addition of SDS results in erratic peak current readings indicating an impairment of the electrode performance. The addition of increasing DTAB and DTAC concentrations causes a decreasing peak current. This suggests that the film of the electrode is corroded or blocked by these surfactants or there are complications with the electron exchange between the analyte and the electrode.

4.2 Gold Electrode.

4.2.1 Chlorogenic Acid Coated Gold Electrode. The results from the study of the detection of hydrazine on CGA coated gold electrode are found below in Table 17 and Figure 41.

Table 17.

Concentration of Hydrazine on CGA Coated Gold Electrode in 0.15M PBS pH 7.5 at scan rate 25 mV/s.

Concentration of Hydrazine (mM)	Ip_a ($x10^{-6}$ A)
0.016	1.27
0.032	1.22
0.048	1.17
0.064	1.14
0.08	1.12
0.096	1.1
0.112	1.07
0.128	1.02

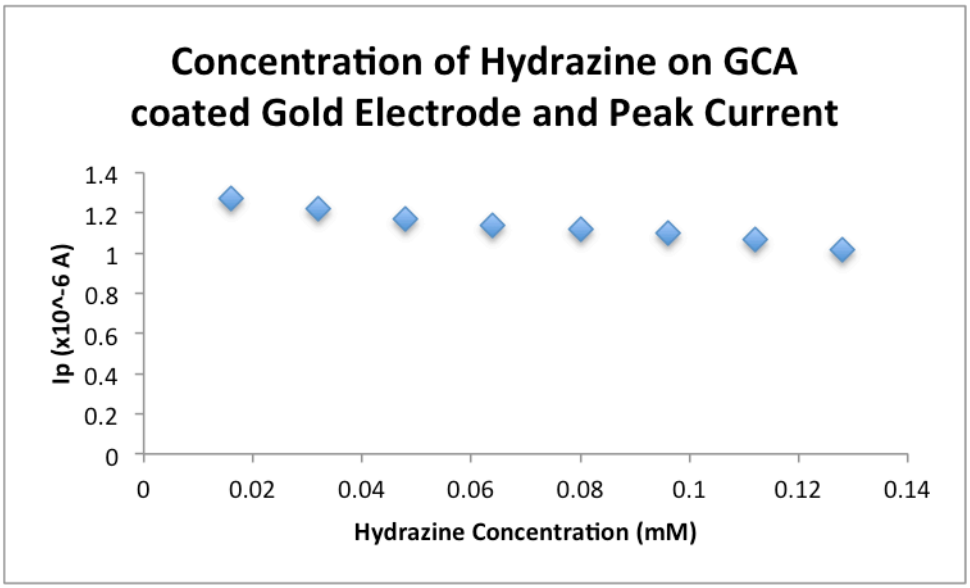

Figure 41. Concentration of Hydrazine on CGA Coated Gold Electrode in 0.15M PBS pH 7.5 at scan rate 25mV/s.

As seen in Figure 41, as analyte is added to the solution for detection, peak current decreases. This is not the expected result and indicates that the CGA film on the gold electrode is compromised and shows little or no detection.

4.2.2 Aspartic Acid Coated Gold Electrode. The results from the study of the detection of nitrobenzene on aspartic acid coated gold electrode are found below in Table 18 and Figure 42.

Table 18.

Concentration of Nitrobenzene on Aspartic Acid Coated Gold Electrode in 0.1M acetic acid buffer pH 5.02 at scan rate 25 mV/s.

Concentration of Nitrobenzene (µM)	Ip_c ($x10^{-6}$ A)
3.3	0.2663
6.6	0.1957
9.9	0.1457
13.2	0.08381
16.5	0.1946
19.8	0.19
23.1	0.1831
26.4	0.08523

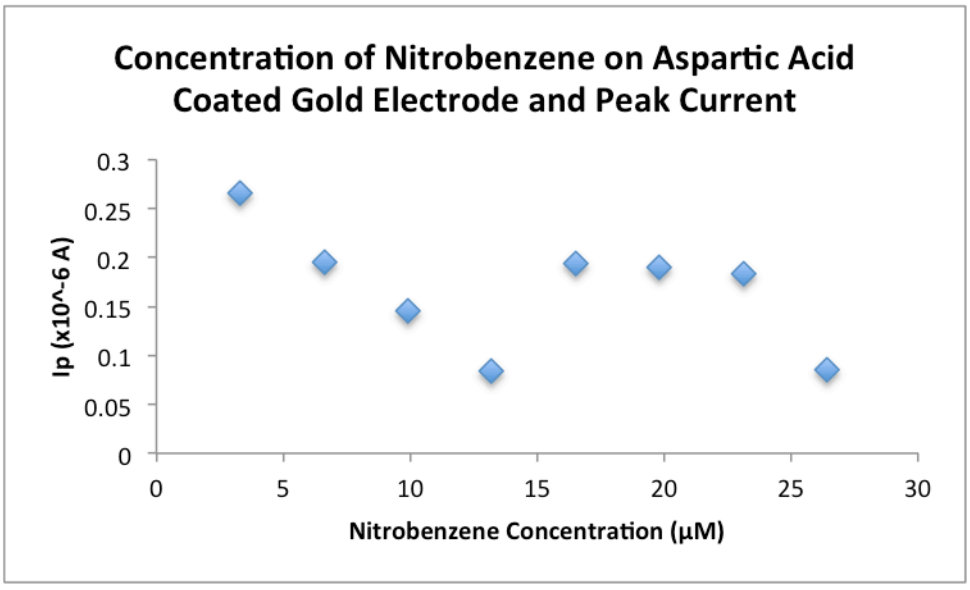

Figure 42. Concentration of Nitrobenzene on Aspartic Acid Coated Gold Electrode in 0.1M acetic acid buffer pH 5.02 at scan rate 25 mV/s.

As seen in Figure 42, the results of this study are erratic and inconclusive. This shows that aspartic acid coated gold electrode is unstable and not suited for use in this study.

4.2.3 Phenol Red Coated Gold Electrode. The results from the study of the detection of nitrobenzene on phenol red coated gold electrode are found below in Table 19 and Figure 43.

Table 19.

Concentration of Nitrobenzene on Phenol Red Coated Gold Electrode in 0.15M PBS pH 7.5 at scan rate 100 mV/s.

Nitrobenzene Concentration (µM)	Ip_c ($x10^{-6}$ A)
3.3	0.02659
6.6	0.02171
9.9	0.02481
13.2	0.03435
16.5	0.04364
19.8	0.03775
23.1	0.03959
26.4	0.04225

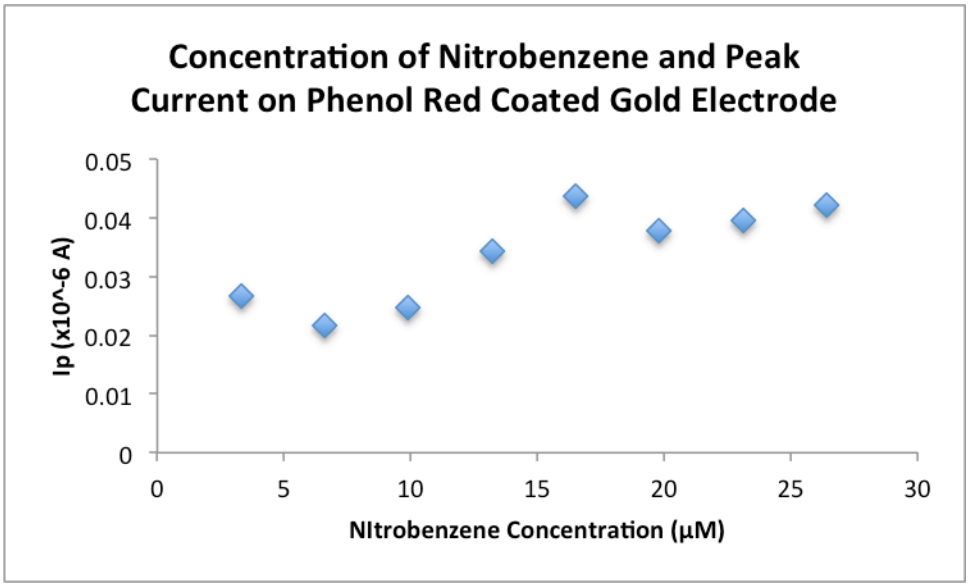

Figure 43. Concentration of Nitrobenzene on Phenol Red Coated Electrode in 0.15M PBS pH 5.02 at scan rate 25mV/s.

As seen in Figure 43, the results of this study are erratic and inconclusive. This indicates that phenol red coated gold electrode is unstable and it was consequently not used in this study.

4.3 Durability of Electrode Coating.

Serial scans were run on each coated electrode with a sample of each analyte to test the durability of the electrode coating. The results of each study are detailed below.

4.3.1 Durability of CGA Coated Electrode with 0.33mM Hydrazine. Table 20 and Figure 44 show the effect of the repetitive scans on the durability of CGA coated electrode with 0.33mM hydrazine.

Table 20.

Durability of CGA Film in 0.15M PBS pH 7.5 at 25mV/s.

Trial	Ip_a ($x10^{-6}$ A)
1	1.288
2	1.42
3	1.414
4	1.192
5	1.155
6	1.043
7	0.9525
8	0.9595
9	1.378
10	0.9559
11	0.8828
12	0.9016
13	0.768
14	0.7294
15	__

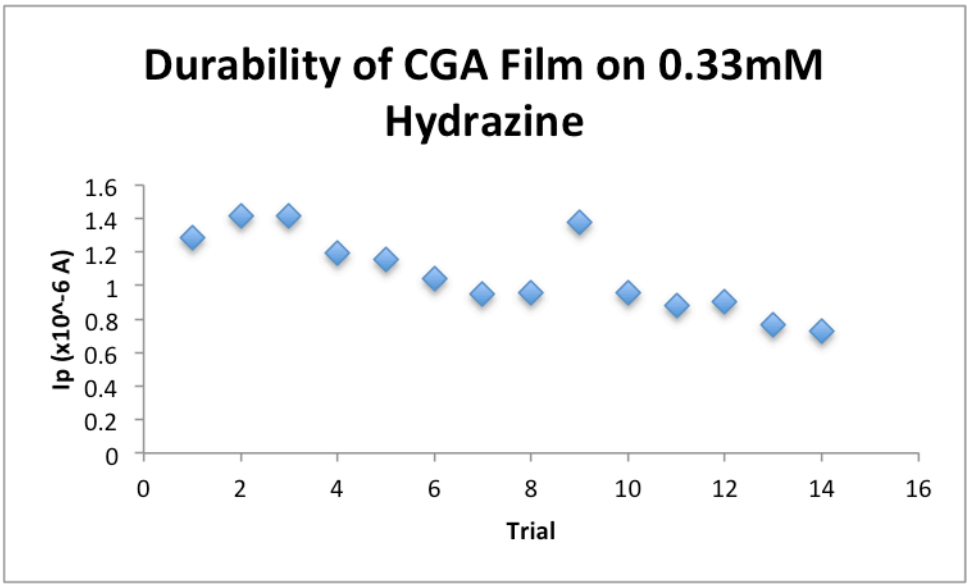

Figure 44. Durability of CGA film on GCE in 0.15M PBS pH 7.5 at scan rate 25mV/s.

Figure 44 shows a decline in peak current suggesting a decomposing of the CGA film. Table 25 shows that after 14 scans of declining function, the electrode was no longer able to detect the analyte.

4.3.2 Durability of Aspartic Acid Coated GCE. Table 21 and Figure 45 show the effect of repetitive scans on the durability of aspartic acid coated electrode with 3.3 µM Nitrobenzene.

Table 21.

Durability of aspartic acid film on GCE in 0.1M acetic acid buffer pH 5.02 at scan rate 25mV/s.

Trial	Ip_c ($x10^{-7}$ A)
1	1.385
2	1.834
3	1.826
4	1.71
5	1.683
6	1.661
7	1.601
8	1.549
9	1.079
10	1.214
11	1.279
12	1.377
13	1.256
14	1.195
15	1.287
16	1.183
17	1.043
18	1.001
19	0.9429
20	0.8962
21	0.8756
22	0.8346
23	0.7683
24	0.709
25	0.685

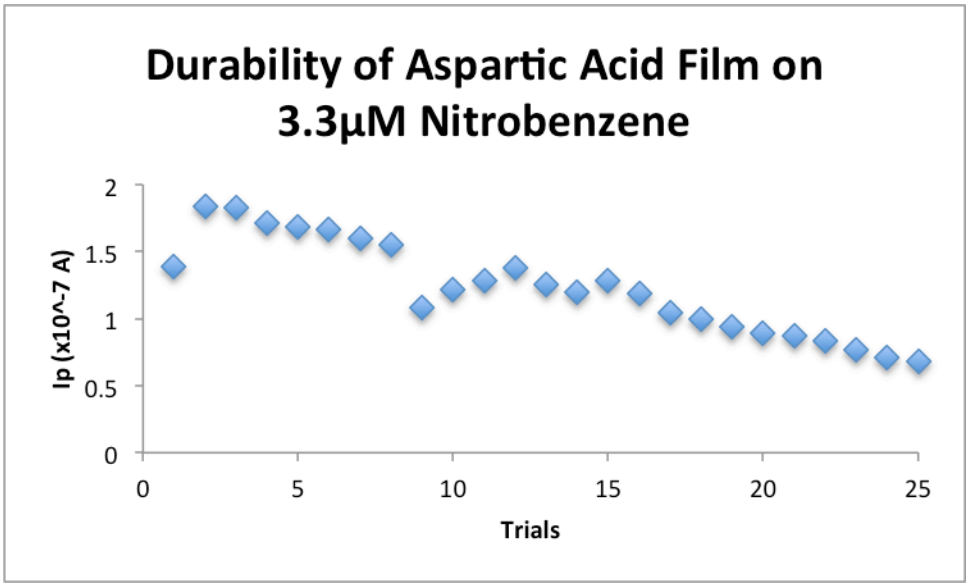

Figure 45. Durability of aspartic acid film on GCE in 0.1M acetic acid buffer pH 5.02 at scan rate 25 mV/s.

A distinct decrease in the peak current as the trials are carried out is seen in Figure 45. There are some points between trials 9 and 15 that appear to be random and suggest more studies need to be done to determine the durability of this film. Overall, the aspartic acid coating on the GCE performance appears to decline in the detection of nitrobenzene. However, the electrode would function reasonably well for 5-8 runs.

4.3.3 Durability of Phenol Red Coated GCE. Table 22 and Figure 46 show the effect of repetitive scans on the durability of phenol red coated electrode with 3.3 µM Nitrobenzene.

Table 22.

Durability of Phenol Red Film in 0.15M PBS pH 6 at 100mV/s with 3.3μM nitrobenzene.

Trial	Ip_c ($x10^{-6}$ A)
1	1.375
2	1.666
3	1.573
4	1.525
5	1.498
6	1.465
7	1.441
8	1.449
9	1.431
10	1.436
11	1.433
12	1.46
13	1.48
14	1.465
15	1.462
16	1.452
17	1.448
18	1.382
19	1.421
20	1.44
21	1.439
22	1.354
23	1.307
24	1.312
25	1.317

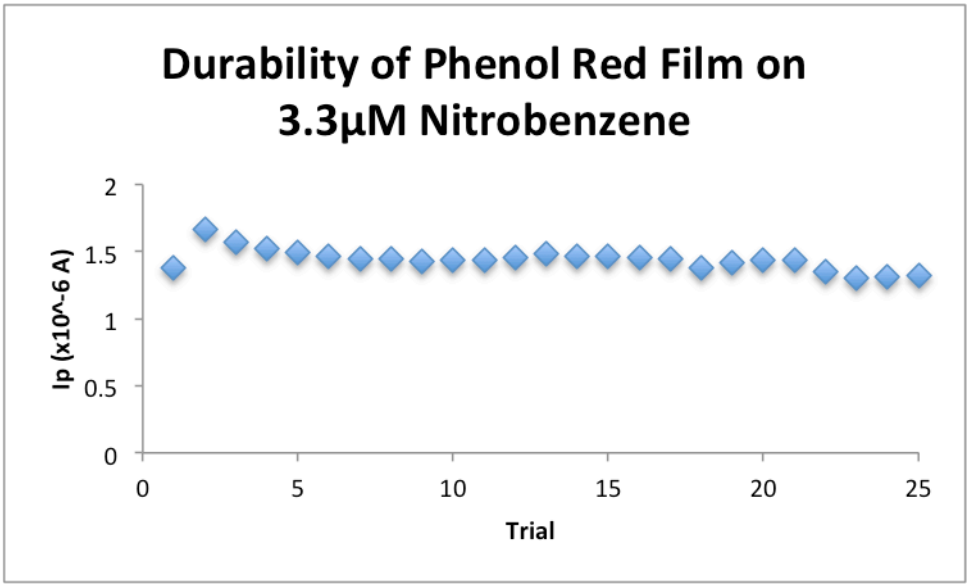

Figure 46. Durability of Phenol Red Film in 0.15M PBS pH 6 at 100mV/s with 3.3µM nitrobenzene.

As shown in Table 22, there is reasonably good precision between the fifth and the 21st run, showing a deviation of 7.7x10^{-7} A. The results for the first four runs could be due to the fact that stability on the electrode surface was not attained. It is therefore observed that the stability of phenol red GCE makes it suitable for the detection of nitrobenzene. This stability may qualify the electrode for field or on-site work.

CHAPTER 5

Discussion and Future Research

5.1 Gold Electrode.

As seen in Figures 41, 42, and 43, the use of a coated gold electrode yields erratic results. Therefore, gold electrode was not further studied in this investigation.

5.2 Chlorogenic Acid Coated GCE for the Detection of Hydrazine.

CGA modified GCE was successful in detecting hydrazine in concentrations as low as 0.05mM, which is in agreement with the lowest detected concentration reported by S.M Golabi and H.R. Zare.[16a] The linear relationship between hydrazine concentration and peak current suggests an adsorption-controlled process.

A pH of 7.5 was selected for use based from previous use reported in literature, yet it is unclear if this is the optimal pH for electrode performance due to lack of data in this study. Further investigation into this study could provide better results.

The highest scan rate that can be used to successfully detect hydrazine on CGA coated GCE is 100mV/s. Our investigation that shows the square root of the scan rate versus the peak current relationship with a linear regression of 0.98427, indicating high redox properties of this electrochemical reaction.

Three surfactants, SDS, DTAC and DTAB were added to the electrochemical cell. The addition of surfactant caused a decrease in peak current, which suggests an interruption in the electron exchange process of the system and consequently and inhibition of electrode function.

5.3 Aspartic Acid Coated GCE for the Detection of Nitrobenzene.

Aspartic acid coated GCE was successful in detecting nitrobenzene in concentrations as low as 3.3μM. The linear relationship between nitrobenzene concentration and peak current suggests an adsorption-controlled detection.

A pH of 5.02 provided the strongest correlation between concentration and peak current and thus most stable electrode performance.

The highest scan rate that was successful in detecting nitrobenzene on aspartic coated GCE was 100mV/s. The plot of square root of the scan rate versus the peak current relationship with a linear regression of 0.99153 indicates high redox properties of this electrochemical reaction.

An addition of surfactants, namely SDS and DTAC, caused a decrease in peak current, which indicates an interruption in the electron exchange process of the system and consequently and inhibition of electrode function. Conversely, the addition of DTAB cause little disruption to the electrode performance.

5.4 Phenol Red Coated Electrode for the Detection of Nitrobenzene.

Phenol red coated GCE was successful in detecting nitrobenzene in concentrations as low as 3.3μM. The linear relationship between nitrobenzene concentration and peak current suggests an adsorption-controlled detection.

A pH of 6 provided the strongest correlation between concentration and peak current and thus most stable electrode performance. At a pH 5 the highest sensitivity of the electrode to nitrobenzene was obtained. A pH in the 5 to 6 range would give the maximum electrode performance.

The highest scan rate that was successful in detecting nitrobenzene on aspartic coated GCE was 130mV/s. The plot of the square root of the scan rate versus the peak current relationship with a linear regression of 0.9559 indicats moderate redox properties possibly inhibited by the pH of the study, 7.5.

On this type of electrode, it is concluded that the addition of surfactant caused a decrease in peak current, which indicates an inhibition in the electron exchange process of the system and consequently a decrease in sensitivity to detect nitrobenzene.

5.5 Aspartic Acid Coated Electrode for the Detection of 4-Nitrotoluene.

Aspartic acid coated GCE was successful in detecting 4-nitrotoluene in concentrations as low as 1.3μM. A linear relationship between 4-nitrotoluene concentration and peak current suggests the feasibility of quantitative analysis at a low detection limit of 4-nitrotoluene.

A pH of 5.02 gives the strongest correlation between concentration and peak current, while pH 6.48 give the most stable sensitivity. A pH within this range would then yield the best electrode performance.

The highest scan rate that was successful in detecting 4-nitrotoluene on aspartic coated GCE was 100mV/s. The plot of square root of the scan rate versus the peak current relationship with a linear regression of 0.98209 indicats high redox properties of this electrochemical reaction.

The presence of surfactants SDS, DTAC and DTAB did not enhance detection. Our study shows that the addition of SDS caused the peak current results to be erratic and DTAC and DTAB caused a decrease in peak current, which shows that the addition of surfactants to the system is unsuitable.

5.6 Film durability.

5.6.1 CGA Coated Electrode for the Detection of Hydrazine. There was an overall steady decline in electrode function as successive scans were conducted. After 14 scans, the electrode ceased ability to detect the analyte. This suggests that the film is unstable after coating for 32 segments.

5.6.2 Aspartic Acid Coated Electrode for the Detection of Nitrobenzene. The aspartic acid film is able to detect analyte at up to 25 scans, but an overall decline in the peak current and consequently the performance is observed. This suggests that the film is unstable after coating for 20 segments.

5.6.3 Phenol Red Coated Electrode for the Detection of Nitrobenzene. The phenol red film is relatively stable until about 15 scans, at which point a more rapid decline in function is observed. The high durability suggests this technique could be developed for field work.

5.7 Future Research.

Future research could be conducted on impedance and film thickness of each coated electrode to determine the best film thickness for electrode performance.

References

1. Ju, K.-S. P., Rebecca E., *Microbiology and Molecular Biology Reviews* **2010,** *74* (2).
2. Singh, S., *J. Hazard. Mater.* **2007,** *144*.
3. (a) Chen, J.-C. S., Jiun-Le; Liu, Chi-Ho; Kuo, Mei-Yuch; Zen, Jyh-Myng, *Anal. Chem.* **2006,** *78*; (b) Ibid, *J. Hazard. Mater.* **2007,** *144*; (c) Krausa, M. S., K., *J. Electroanal. Chem.* **1991,** *461*; (d) Senesac, L. J., T.G., *Mater. Today* **2008,** *11*; (e) Wang, J., *Anal. Chim. Acta* **2003,** *507*; (f) Yanghai, G. C., Xie; Jaiqiang, Xu; Guqing, Wang, *J. Hazard. Mater.* **2009,** *164*.
4. Hable, M. S., C; Asowala, C.; Williams, K., *J. Chromatogr. Sci.* **1991,** *29*.
5. (a) Brittain, T. B., R.; Greenwood, C.; Thomson, A.J., *Eur. J. Biochem.* **1992,** *209*; (b) Frenzel, W. S.-B., J.; Zinvirt, B., *Talanta* **2004,** *64*; (c) Glustanin, D. D.-D., I.; Colombo, R.; Milzani, A.; Rossi, R., *Free Radical Res.* **2004,** *38*.
6. (a) Ladbeck, R. S. K., P.; Karst, U., *Anal. Chem.* **2003,** *75*; (b) Rose, A. Z., Z.; Madigan, C.F.; Swazer, T.M.; Bulovic, V., *Nature* **2005,** *435*; (c) Walleborg, S. R. B., C.G., *Anal. Chem.* **200,** *72*.
7. (a) Bogue, R. W., *Sensor Review* **2000,** *24*; (b) De Lucia, F. C. J. H., R.S.; McNesby K.L.; Winkel, Jr., R.J; and Miziolak, A.W., *Appl. Opt.* **2003,** *42*.
8. (a) Cai, X. a. Z., Z, *J. Electroanal. Chem.* **1988,** *252*; (b) Newby, J. E. d. H., M.P.L., *Analyst* **1985,** *110*; (c) Obirai, J. a. N., T., *J. Electroanal. Chem.* **2004,** *573*; (d) Wen, Z. H. K., T.F., *Talanta* **2004,** *61*.
9. (a) Furton, K. G. M., I.J., *Talanta* **2001,** *54*; (b) Harper, R. J. A., K.G., *Talanta* **2005,** *67*.
10. Wang, J., *Analytical Electrochemistry*. 2nd ed.; Wiley: 2000.

11. Organization, W. H. Enviormental Health Criteria 68 Hydrazine. http://www.inchem.org/documents/ehc/ehc/ehc68.htm - PartNumber:2.

12. Lonza Propellants-Product Applications. http://www.archchemicals.com/Fed/HDR/Products/Propellants/prodapps.htm.

13. EPA Hydrazine. http://www.epa.gov/ttn/atw/hlthef/hydrazin.html - ref3.

14. Medicine, N. L. o. 4-Nitrotoluene. http://toxnet.nlm.nih.gov/cgi-bin/sis/search/r?dbs+hsdb:@term+@rn+@rel+99-99-0.

15. Organization, W. H. Nitrobenzene. http://www.inchem.org/documents/ehc/ehc/ehc230.htm.

16. (a) S.M. Golabi, H. R. Z., Electrocatalytic oxidation of hydrazine at a chlorogenic acid (CGA) modified glassy carbon electrode. *J. Electroanal. Chem.* **1999,** *465* (1999), 168-176; (b) Warrington, R. J.; Higson, S. P., Polymer modified electrodes for the reversible oxidation-reduction of NAD+/NADH for use within amperometric biosensors. (0067-8856 (Print)); (c) Zhang, L.; Lin, X., Electrochemical behavior of a covalently modified glassy carbon electrode with aspartic acid and its use for voltammetric differentiation of dopamine and ascorbic acid. *Anal Bioanal Chem* **2005,** *382* (7), 1669-1677.

17. Salimi, A. H., Rahman; Ghadermazi, Mohammad, *Talanta* **2005,** *65*.

18. Xiao-GangWang, Y.-J. F. Z.-X. H. L.-H. G., *J. Electrochem. Soc.* **2010,** *46* (12).

19. Gongjun, Y. X., Qu; MingShen, Chengyn; Wang, Quishuqu; Xiaoya, Hu, *Michrochimica acta* **2008,** *160*.

20. Xian-Gang, Q.-S., Wang-Zhuan Liu, Ya-Ping, Ding, *Electrochim. Acta* **2006,** *52*.